

A Differential Representation of Cosmological Wavefunctions

Aaron Hillman^{1,*} and Enrico Pajer^{2,†}

**Department of Physics, Princeton University, Washington Road, Princeton, NJ, USA*

† Department of Applied Mathematics and Theoretical Physics, University of Cambridge, Wilberforce Road, Cambridge, CB3 0WA, UK

Our understanding of quantum field theory rests largely on explicit and controlled calculations in perturbation theory. Because of this, much recent effort has been devoted to improve our grasp of perturbative techniques on cosmological spacetimes. While scattering amplitudes in flat space at tree level are obtained from simple algebraic operations, things are harder for cosmological observables. Indeed, computing cosmological correlation functions or the associated wavefunction coefficients requires evaluating a growing number of nested time integrals already at tree level, which is computationally challenging. Here, we present a new “differential” representation of the cosmological wavefunction in de Sitter spacetime that obviates this problem for a large class of phenomenologically relevant theories. Given any tree-level Feynman-Witten diagram, we give simple algebraic rules to write down a seed function and a differential operator that transforms it into the desired wavefunction coefficient for any scale-invariant, parity-invariant theory of massless scalars and gravitons with general boost-breaking interactions. In particular, this applies to large classes of phenomenologically relevant theories such as those described by the effective field theory of inflation or solid inflation. Trading nested bulk time integrals for derivatives on boundary kinematical data provides a great computational advantage, especially for processes involving many vertices.

¹aaronjh@princeton.edu

²enrico.pajer@gmail.com

Contents

1	Introduction	2
2	Overview	4
3	Step 1: The seed flat-space wavefunction ψ^{flat}	10
3.1	Examples	12
4	Step 2: The intermediate wavefunction ψ_{int}	14
4.1	Motivation	15
4.2	The general case	16
4.3	Examples	18
5	Step 3: The final de Sitter wavefunction ψ	21
5.1	General properties	22
5.2	Examples	24
6	Minimal coupling to gravity	29
6.1	Contact diagrams	30
6.2	Exchange Diagrams	31
6.3	Example: Scalars exchanging a graviton	33
6.4	Example: Gravitons exchanging a graviton	35
7	Conclusions and outlook	36
A	Derivation of Propagator Relations	37

1 Introduction

At the heart of our current cosmological paradigm sits the observation that the distributions of everything we observe on cosmological scales, from galaxies to dark matter, from neutrinos to photons, was seeded by quantum fluctuations during a primordial phase that preceded the hot big bang. To make predictions for cosmological surveys requires computing the statistics of these fluctuations using quantum field theory in curved spacetime and accounting for the quantum behavior of spacetime (metric) fluctuation. A main driver for this line of research is the expectation that current or future cosmological datasets will shed light on new physics beyond the standard model and perhaps the perturbative regime of quantum gravity.

The workhorse of this program is perturbation theory, which has been used extensively in the past two decades to compute predictions for a variety of models and classes of theories. On the one hand, perturbation theory gives us with a very rich set of explicit and phenomenologically useful results and predictions. On the other hand, it is also a springboard to the exploration of deeper non-perturbative structures. For example, much of our understanding of non-perturbative results in quantum field theory rests on extrapolating the observed behavior in perturbation theory. One example are positivity bounds [1], where we extrapolate the analytic structure of perturbation theory to the UV-completion of effective field theories and use it to discriminate theories that can be extended to arbitrarily high energies in a consistent way. Another example is the S-matrix numerical bootstrap approach to the calculation of non-perturbative amplitudes (see e.g. [2]). These successes in the study of flat-space observables motivated a recent resurgence in the study of *perturbation theory* on de Sitter and cosmological spacetimes [3–30] which builds upon many results obtained over the past twenty years [31–36]. One of the eventual goals of this program is deriving cosmological positivity bounds³ and a non-perturbative cosmological bootstrap (see [23, 25, 44] for progress in this direction).

In this work, we derive a new representation of tree-level wavefunction coefficients for massless scalars and gravitons to any order in perturbation theory. We call this a “differential representation” because the wavefunction coefficients are obtained by acting with differential operators on a class of simple seed functions, which in turn are determined by purely algebraic rules. Our differential representation covers all boost-breaking interactions that appear in phenomenological models of inflation and dark energy, as for example in the effective field theory of inflation [45–47] or solid inflation [48]. Following the hint of cosmological observations, we assume scale invariance throughout our work, but we neglect the small deviation implied by the measured scalar spectral tilt. In practice, given a certain Feynman-Witten diagram in dS, where interactions are specified for each vertex, our differential representation generates a seed function and a differential operator that acts on it to give the associated wavefunction coefficient. All differential operators act on the external spatial momenta of the Fourier-space wavefunction coefficient and consequently the notion of time in the bulk of de Sitter completely disappears from the calculation. This representation turns out to be much simpler than the lengthy calculation of nested time integrals

³Several constraints have been derived in flat space for boost-breaking effective theories that capture in the sub-Hubble limit of common models of inflation and dark energy, see e.g. [37–43].

and even much more compact than the result of those integrals. The consequent improvement in calculation time is already remarkable for a single exchange diagram and grows exponentially with the number of internal legs. For example, we show that the differential representation of a five-point function with three cubic ϕ^3 couplings and two internal lines (three-site chain) is contained in less than a line. For the reader familiar with our results, this can be computed with pen and paper in minutes, while performing the corresponding time integrals in the standard bulk-representation requires much longer with an off-the-shelf software such as Mathematica on a standard CPU.

The rest of the paper is organized as follows. For the reader interested in using our results in practical calculations, in Section 2 we give a brief summary of our three-step procedure to derive the differential representation of any tree-level contribution to the n -th wavefunction coefficient ψ_n for a massless scalar field in de Sitter. The following three sections provide a derivation of each of the steps of this procedure, as depicted in Figure 1, and a number of practical examples. In particular, in Section 3, we introduce the seed wavefunction ψ^{flat} , which is the wavefunction of a massless scalar with polynomial interactions in flat spacetime (Step 1). Then, in Section 4, we derive the differential operator that acting on ψ^{flat} gives us an intermediate wavefunction ψ_{int} , which accounts for the difference in mode functions between flat spacetime and de Sitter (Step 2). At the level of the bulk time integral, this step correctly reproduces the integrand modulo overall powers of conformal time at each vertex. The last step is discussed in Section 5 and consists of fixing the correct overall powers of conformal time at each vertex as well as adding the appropriate momentum factors to the vertices and the external legs, yielding the final de Sitter wavefunction ψ (Step 3). In Section 6 we discuss the extension of our procedure to include massless gravitons and the interactions of minimal coupling to gravity with two explicit examples. We conclude in Section 7 with a discussion and an outlook. Appendix A contains the computational details of relations obeyed by propagators that we use in the bulk of the paper.

While this paper was (slowly) being completed, reference [49] appeared, which also develops the idea of relating the dS wavefunction to flat spacetime objects with differential operators.

Notation and conventions We will use the following de Sitter line element (in mostly positive signature)

$$ds^2 = -dt^2 + a^2 dx^i \delta_{ij} dx^j = \frac{-d\eta^2 + dx^i \delta_{ij} dx^j}{H^2 \eta^2}, \quad (1.1)$$

with scale factor $a = e^{Ht} = -1/(H\eta)$.

Our bulk-to-bulk propagator G has an overall factor of i , schematically $G \sim iPKK$ (see (3.3)). With this convention the Feynman rules are that every internal line corresponds to a G , there is an overall i for every diagram, and vertices do not get any i , for example the vertex of $g\phi^3/3!$ is simply g .

We use \mathbf{k} and $k = |\mathbf{k}|$ for *external momenta* labelled by letters in the first half of the latin alphabet, $a, b = 1, \dots, n$ for an n -point function. The I *internal momenta* are denoted by \mathbf{p}_m and their energy is $p_m = |\mathbf{p}_m|$ with $m = 1, \dots, I$. Finally, the $V = I + 1$ vertices have valency $n_A \geq 3$

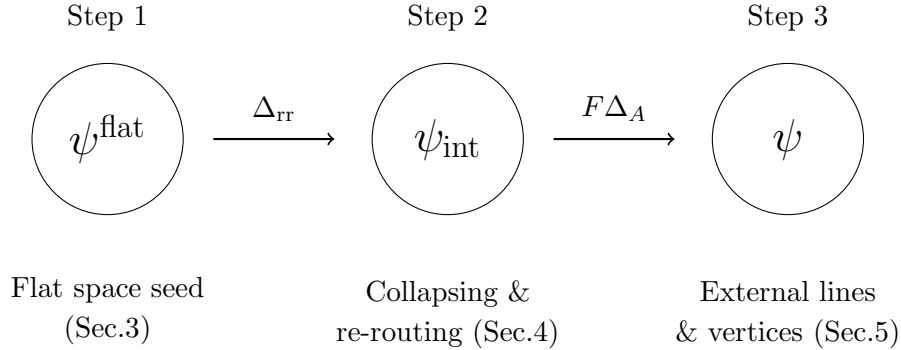


Figure 1: Depiction of the sequence of differential operators acting on the flat space seed function ψ^{flat} to obtain the function ψ specified by the edges and vertices.

(the number of external and internal legs ending on the vertex) and are placed at conformal time η_A with $A = 1, \dots, V$. The sum of energies k_a running from a single vertex A to the boundary is denoted by $q_A = \sum_{a \in A} k_a$.

The wavefunction for some future boundary configuration of a field $\Phi(\vec{x})$ is given by a path integral and is naturally organized as

$$\Psi[\Phi] = \exp \left\{ - \sum_n \frac{1}{n!} \int \left[\prod_i^n \frac{d^3 k_i}{(2\pi)^3} \Phi(\mathbf{k}_i) \right] \psi_n (2\pi)^3 \delta^3 \left(\sum \mathbf{k}_a \right) \right\}. \quad (1.2)$$

The delta-function stripped ψ_n 's are the wavefunction coefficients we are interested in computing and can be defined as

$$(2\pi)^3 \delta^{(3)} \left(\sum_i \vec{k}_i \right) \psi_n = \left. \frac{\delta^n \Psi}{\delta \Phi(\mathbf{k}_1) \dots \delta \Phi(\mathbf{k}_n)} \right|_{\Phi=0}. \quad (1.3)$$

These can be computed in perturbation theory using Feynman-Witten rules. We will indicate by ψ_n the wavefunction coefficients in de Sitter, while ψ_n^{flat} is reserved for the wavefunction coefficients in flat spacetime of a theory with only polynomial interactions (see Sec. 3). The kinematic dependence of ψ^{flat} can be parameterized in terms of the combinations q_A for each vertex A and the edge energies p_m . Therefore, instead of writing $\psi^{\text{flat}}(k_1, \dots, k_n)$, we will use the notation $\psi^{\text{flat}}(q_1, \dots, q_V; p_1, \dots, p_I)$, where V is the number of vertices and I the number of edges. In general ψ^{flat} depends on the internal energies p , but we will always omit this dependence when no ambiguity arises.

2 Overview

In this section, we give an overview of our procedure to compute the cosmological wavefunction for any given tree-level diagram for a massless scalar field in de Sitter with arbitrary boost-breaking local interactions that respect scale invariance. In particular our approach does not rely on invariance under de Sitter boosts and can be applied for example to any of the interactions

resulting from the Effective Field Theory of Inflation [45, 46]. Our procedure consists of three steps. In Step 1 we start from a seed wavefunction ψ^{flat} that can be computed *algebraically* using the results of [3]. These functions are determined by the topology of the amputated diagram i.e. the diagram defined by only the internal lines (edges). Depending on the details of the interactions, additional ψ^{flat} 's diagrams are needed corresponding to different ways of collapsing internal lines. In Step 2 we give a prescription to write down a derivative operator that acts on ψ^{flat} and accounts for the structure of the exchange propagators up to overall powers of conformal time in the integrand. Finally, in Step 3 we fix the correct power of conformal time at each vertex and account for external kinematical factors coming from spatial derivatives and polarization tensors.

In its first and most basic implementation, our approach works only for interactions with enough derivatives to cancel all inverse powers of η present in the measure of covariant spacetime integrals. More precisely, we start by considering vertices that satisfy the following criterion

$$d \equiv 2n_{\partial_t} + n_{\partial_i} \geq 4, \quad (2.1)$$

where n_{∂_t} and n_{∂_i} are the number of time and spatial derivatives, respectively. For scalar perturbations this is not a very strong restriction. For example, we know that the largest interactions in a generic model of single-field inflation can be captured by the decoupling limit of the EFT of inflation, where a shift symmetry is imposed on the Goldstone boson of time translations. The leading interactions relevant for the bispectrum are $\dot{\phi}^3$ and $\dot{\phi}\partial_i\phi^2$, which in turn lead to equilateral and orthogonal non-Gaussianities [50]. Both of these interactions satisfy the above criterion and so do all the shift symmetric operators contributing to quartic and higher interactions. Later, in Section 6, we will show that the restriction in (2.1) can be relaxed in certain cases, such as the minimal coupling to gravity. In the following we summarize the three steps involved in deriving the differential representation of the dS wavefunction.

Step 1: The seed functions from flat spacetime The first step consists in computing the wavefunction coefficient in Minkowski for a theory with purely polynomial interactions. A simple and purely algebraic prescription to write down this “seed” function ψ^{flat} without explicitly performing any time integral was described in [3] and we review it in detail in Section 3. Any tree-level wavefunction coefficient ψ_V^{flat} is represented by a tree diagram with V vertices and $I = V - 1$ internal lines (edges). To every vertex $A = 1, \dots, V$ we associate a total external energy q_A , while to every edge $m = 1, \dots, I$ we associate an internal energy p_m . The algebraic computation of ψ^{flat} is based on the following recursive relation

$$\left(\sum_A^V q_A \right) \psi_V^{\text{flat}} = \sum_m^I \psi_{V'}^{\text{flat}}(q_1, \dots, q_B + p_m, \dots, q_{n'}) \psi_{V-V'}^{\text{flat}}(q_1, \dots, q_{B'} + p_m, \dots, q_{n-n'}) \quad (2.2)$$

where the sum runs over all edges $m = 1, \dots, I$ and $0 < V' < V$ is the number of vertices left in one of the two subdiagrams when the m -th edge connecting vertices B and B' is removed (see (3.9) for a graphical representation)⁴. Our analysis is restricted to tree level and so we have

⁴ V of course does not uniquely define a topology for $V > 3$ and it is implied that we have the graphs induced by the original graph when cut on edge m . This is made clear in (3.9).

omitted the loop-deletion term in the above recursion. From this relation we can easily write down all desired ψ^{flat} starting from the trivial $V = 1$ base case. For example⁵:

$$\psi_1^{\text{flat}}(q) = \frac{1}{q}, \quad (2.3)$$

$$\psi_2^{\text{flat}}(q_1, q_2; p) = \frac{\psi_1^{\text{flat}}(q_1 + p)\psi_1^{\text{flat}}(q_2 + p)}{q_1 + q_2}, \quad (2.4)$$

$$\psi_3^{\text{flat}}(q_1, q_2, q_3; p_1, p_2) = \frac{\psi_2^{\text{flat}}(q_1, q_2 + p_2)\psi_1^{\text{flat}}(q_3 + p_2) + \psi_1^{\text{flat}}(q_1 + p_1)\psi_2^{\text{flat}}(q_2 + p_1, q_3)}{\sum_A^3 q_A}, \quad (2.5)$$

and so on and so forth.

Step 2: Intermediate Wavefunction In Step 2, a new “intermediate” wavefunction ψ_{int} is obtained from ψ^{flat} by applying a suitable sequence of differential operators that are fully fixed by specifying where time derivatives at each vertex act on an internal bulk-to-bulk propagator. Since each internal line or “edge” is attached to two vertices, it is useful to speak in terms of “half-edges” (see Figure 2) which are uniquely specified by a vertex edge pairing. We may therefore denote a half-edge by a pair of indices mA , where the first index indicates that the half-edge is part of the m edge and the second index indicates that it ends on the vertex A . An half-edge that has no time derivatives is said to be of the ϕ type, while an half-edge with one time derivative is said to be of the ϕ' type. As we are considering interaction vertices with at most one time derivative⁶ there are no other possibilities. Once the two half-edges of a given edge are specified, four options for the corresponding bulk-to-bulk propagators $G(\eta, \eta', p)$ emerge: no time derivatives, which we indicate by $\langle\phi\phi\rangle$, one time derivative, $\langle\phi'\phi\rangle$ or $\langle\phi\phi'\rangle$, or two time derivatives, $\langle\phi'\phi'\rangle$. With these definitions we have⁷

$$\begin{array}{c} \phi \\ \bullet \\ \eta \end{array} \xrightarrow{p} \begin{array}{c} \phi \\ \bullet \\ \eta' \end{array} \quad G_{\phi\phi}(\eta, \eta', p) = G(\eta, \eta', p), \quad (2.6)$$

$$\begin{array}{c} \phi \\ \bullet \\ \eta \end{array} \xrightarrow{p} \begin{array}{c} \phi' \\ \bullet \\ \eta' \end{array} \quad G_{\phi\phi'}(\eta, \eta', p) = \partial_{\eta'} G(\eta, \eta', p), \quad (2.7)$$

$$\begin{array}{c} \phi' \\ \bullet \\ \eta \end{array} \xrightarrow{p} \begin{array}{c} \phi' \\ \bullet \\ \eta' \end{array} \quad G_{\phi'\phi'}(\eta, \eta', p) = \partial_{\eta}\partial_{\eta'} G(\eta, \eta', p). \quad (2.8)$$

⁵Notice that where no confusion arises we indicate explicitly only the dependence of ψ^{flat} on the external energies q_A and leave the dependence on the internal energies p_m implicit.

⁶In perturbation theory, any higher time derivative can always be re-written in terms of at most one time derivative using repeatedly the (non-linear) equations of motion. This procedure also generates contributions to the wavefunction from field redefinitions (we thank S. Jazayeri for pointing this out), which don't have total energy poles and correspond to contact terms in position space. These contributions from field redefinitions are neglected in our analysis. If desired, they can be included straightforwardly with traditional methods.

⁷Here η' is just another name for a time variable. The prime should not be confused with the prime on ϕ , which indicates a time derivative, $\phi' = \partial_{\eta}\phi$.

Given the explicit form of G for fields with the massless de Sitter mode function in (4.2), these propagators obey the following relations to the flat space propagator

$$G_{\phi\phi}(\eta, \eta', p) = \frac{1}{p^2} [(1 - \eta\partial_\eta)(1 - \eta'\partial_{\eta'})G_{\text{flat}}(\eta, \eta', p) + \eta\eta'\delta(\eta - \eta')] , \quad (2.9)$$

$$G_{\phi'\phi'}(\eta, \eta', p) = \eta\eta' [p^2 G_{\text{flat}}(\eta, \eta', p) - \delta(\eta - \eta')] , \quad (2.10)$$

$$G_{\phi\phi'}(\eta, \eta', p) = (1 - \eta\partial_\eta)\eta' G_{\text{flat}}(\eta, \eta', p) = G_{\phi'\phi}(\eta', \eta, p) . \quad (2.11)$$

It is straightforward to keep track of the powers of energy p . This requires multiplying by the factor specified in (2.13). On the other hand, there are two aspects of the above relations that require more work. We have to account for (i) the relative powers of η in the terms of the exchange propagators and (ii) for the δ functions. Issue (i) will be addressed by the operation of *re-routing*. This is a manifestation of integration by parts in terms of a differential operator which captures how the time derivatives get routed out to a boundary vertex. Issue (ii) will be addressed by the operation of *collapsing*. Each term in the sum over ways of collapsing edges will get its own rerouting operator.

Let's start with re-routing. Using integration by parts, the temporal differential operators $(1 - \eta\partial_\eta)$ can be routed out of all time integrals to act on the times of those vertices of the diagram that are only connected to a single internal edge. When acting on these times, the derivatives can be re-expressed as kinematic differential operators on ψ^{flat} . In (2.9)-(2.11) we see that a ∂_η appears for every half-edge ϕ in the diagram. Moreover, as discussed below, we must also sum over diagrams with $\langle\phi'\phi'\rangle$ and $\langle\phi\phi\rangle$ propagators collapsed by the δ -functions. The differential operator Δ_{rr} (“rr” stands for re-routing) which accounts for re-routing $(1 - \eta\partial_\eta)$ on a given ϕ half-edge is (see Figure 2)

$$\begin{cases} \Delta_{\text{rr}} = 1 + \left[\sum_A (1 + q_A \partial_{q_A}) + \sum_m (1 + p_m \partial_{p_m}) \right] & \text{vertex side,} \\ \Delta_{\text{rr}} = 1 - \left[\sum_A (1 + q_A \partial_{q_A}) + \sum_m (1 + p_m \partial_{p_m}) \right] & \text{opposite-vertex side,} \end{cases} \quad (2.12)$$

where the sum runs over all vertices encountered when flowing out of the diagram from the chosen half edge. In general, one needs a Δ_{rr} operator for each ϕ half-edge in the diagram and when necessary we will specify which half-edge Δ_{rr} corresponds to, as e.g. in (6.11), (6.12) and (6.16). The order of application of these differential operators is relevant and can be understood from the integration by parts. Specifically, on a given path out of the diagram, the operator corresponding to the innermost ϕ half-edge should be applied to the seed function ψ^{flat} first. Moreover, when multiple ϕ half-edges are present, choices of flow should not cross. This will be expanded upon in Section 4.

Let's move on to collapsing. Two of the three propagator relations have δ -functions: $G_{\phi\phi}$ and $G_{\phi'\phi'}$. Each δ -function has the effect of collapsing the corresponding edge and merging the two vertices to which that edge was attached. For example a $\delta(\eta_A - \eta_B)$ would merge vertex A at time η_A with external energy q_A with vertex B at time η_B with external energy q_B . In doing

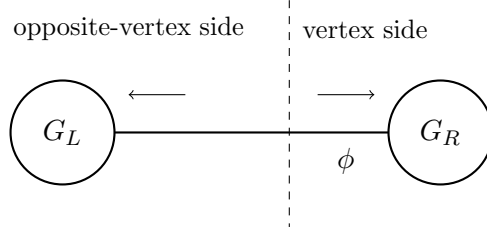


Figure 2: For a half-edge ϕ the graphic defines flowing vertex side or opposite-vertex side. A choice of flow determines a differential operator summing over energies in G_L including the edge itself or in G_R including the vertex.

this we have to be careful with the overall powers of conformal time. The δ -functions in $G_{\phi\phi}$ and $G_{\phi'\phi'}$ have different net powers of conformal time relatively to the non- δ -function terms in each expression. To account for this difference, we count the powers of conformal time in the δ -function terms relatively to the flat-space propagator. For $\phi'\phi'$, the power is the same and therefore the collapsed contribution has merely a minus sign. For $\phi\phi$, the δ -function has two powers of conformal time in excess of term with G_{flat} and therefore collapsing the edge should be accompanied by a single derivative with respect to each of the vertex energies to which the edge is connected, namely $(-i\partial_{q_A})(-i\partial_{q_B})$, or equivalently two derivatives of the energy of the merged vertex. These operations act after the re-routing operators defined below.

Lastly, we account for the power spectrum normalization of a given (in general collapsed) diagram. This factor is merely the product over p_m^2 for each (non-collapsed) $\phi'\phi'$ exchange edge and p_m^{-2} for each (non-collapsed) $\phi\phi$ exchange edge. Equivalently, this is the product over p_m for each ϕ' in the truncated⁸ diagram and p_m^{-1} for each ϕ . We can call this

$$P = \prod_{\phi'\phi'} p_m^2 \prod_{\phi\phi} \frac{1}{p_m^2} \quad (2.13)$$

where the products are over propagators of each type.

Summarizing, in Step 2 each internal propagator requires the following operations

$$\phi'\phi' \rightarrow \text{collapsing}, \quad \phi\phi' \rightarrow \text{re-routing}, \quad \phi\phi \rightarrow \text{collapsing \& re-routing}. \quad (2.14)$$

For every collapsed edge with energy p that merges vertex A and B , the following operator must be applied after the application of re-routing operators:

$$\text{collapsing } \phi\phi \rightarrow -\frac{1}{p^2} \partial_{q_A} \partial_{q_B} \quad \text{collapsing } \phi'\phi' \rightarrow -1. \quad (2.15)$$

Notice that the re-routing operation is not required for the collapsed contribution, it only appears in the non-collapsed contribution. The intermediate wavefunction is comprised of the sum over all

⁸All external lines should be amputated here because they are captured later in Step 3.

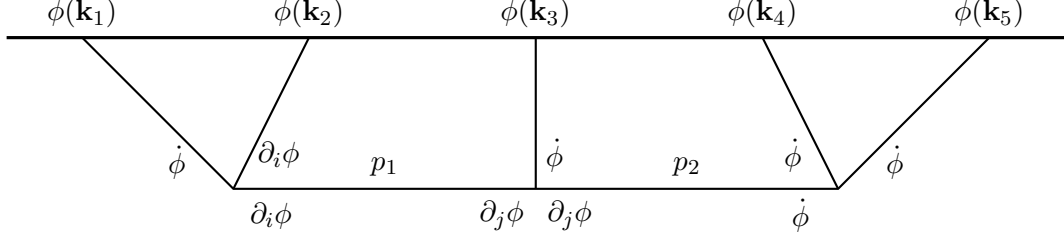


Figure 3: A particular contribution to the quintic wavefunction coefficient from the indicated cubic interactions.

ways of collapsing the relevant propagators and applying the prescribed differential operators on the seed wavefunction in each case. Each diagram in the sum over collapsing should be multiplied by the associated P-factor (2.13).

Step 3: Final de Sitter Wavefunction In the final step we derive the desired de Sitter wavefunction coefficient. We now specify the precise structure of the vertices and bulk-to-boundary propagators, not merely the skeleton and structure of the internal lines (a.k.a. bulk-to-bulk propagators). To this end, we apply derivatives with respect to the vertex energies appearing in the bulk-to-boundary propagators, we add factors of k_a^2 or $(1 - k_i \partial_{k_i})$ to reproduce the external massless bulk-to-boundary mode functions with one time-derivative (K') or no time-derivatives (K), respectively. In particular, for every vertex we apply the following operator (see Sec 5)

$$\Delta_A = i^{4-d_A} \left(\prod_{a \in K'} k_a^2 \right) \left(\prod_{b \in K} (1 - k_b \partial_{q_b}) \right) \frac{\partial^{d_A-4}}{\partial q_A^{d_A-4}}, \quad (2.16)$$

where d_A was defined in (2.1).

We also account for all contractions of spatial momenta and polarization tensors by adding a multiplicative factor F . In summary, the final de Sitter wavefunction coefficient is given by

$$\psi = F \left(\prod_A \Delta_A \right) \psi_{\text{int}}. \quad (2.17)$$

Featured examples Now we present two examples to illustrate the application of the above prescription. In the first example, we will calculate the contribution coming from the diagram depicted in Fig. 3. This does not represent the full contribution at this order in the couplings; that will be presented in Section 5. Nonetheless, this example illustrates the essential content of the prescribed rules.

The relevant seed functions are

$$\psi_3^{\text{flat}}(q_1, q_2, q_3; p_1, p_2) = \frac{1}{q_T(q_1 + p_1)(q_3 + p_2)(q_2 + p_1 + p_2)} \left(\frac{1}{q_1 + q_2 + p_2} + \frac{1}{q_3 + q_2 + p_1} \right), \quad (2.18)$$

$$\psi_2^{\text{flat}}(q_1 + q_2, q_3; p_2) = \frac{1}{q_T(q_1 + q_2 + p_2)(q_3 + p_2)}, \quad (2.19)$$

where $q_1 = k_1 + k_2$, $q_2 = k_3$, $q_3 = k_4 + k_5$ and $q_T = q_1 + q_2 + q_3$. The intermediate wavefunction is then (see (4.20))

$$\begin{aligned} \psi_{\text{int}} = \frac{1}{p_1^2} (2 + q_1 \partial_{q_1}) (-1 - p_1 \partial_{p_1} - q_1 \partial_{q_1}) (4 + q_2 \partial_{q_2} + p_1 \partial_{p_1} + q_1 \partial_{q_1}) \psi_3^{\text{flat}} \\ - \frac{1}{p_1^2} \partial_{q_1} \partial_{q_2} (2 + q_1 \partial_{q_1}) \psi_2^{\text{flat}}. \end{aligned} \quad (2.20)$$

Finally the desired contribution to the dS wavefunction coefficient is

$$\psi = -(\mathbf{p}_1 \cdot \mathbf{k}_2)(\mathbf{p}_1 \cdot \mathbf{p}_2)(k_1 k_3 k_4 k_5)^2 (1 - k_2 \partial_{q_1}) \partial_{q_3}^2 \psi_{\text{int}}. \quad (2.21)$$

In the second example, we provide a simple formula for *any* tree-level diagram with n external legs, V vertices and $I = V - 1$ internal lines in a theory where all interactions are of the form ϕ^n for some integer $n \geq 3$. The corresponding contribution to the dS wavefunction coefficient ψ_n is given by

$$\psi_n = \prod_{a=1}^n k_a^2 \prod_{A=1}^V (-1)^{n_A} \partial_{q_A}^{2n_A-4} \sum_{\text{collapsings}}^{2^I} \left[(-1)^{n_c} \psi_{n-n_c}^{\text{flat}} \prod_m^{I-n_c} p_m^2 \right], \quad (2.22)$$

where the sum is over the 2^I possible ways to collapse a number $0 \leq n_c \leq n$ of internal lines and the product goes over the $I - n_c$ un-collapsed internal lines. Here n_A is the valency of each ϕ^{n_A} interaction and the arguments of the seed wavefunctions ψ^{flat} are determined by the specific collapsing under consideration.

3 Step 1: The seed flat-space wavefunction ψ^{flat}

In this section, we discuss the seed function ψ^{flat} and review the simple algebraic prescription derived in [3] to compute it for any tree-level diagram⁹.

Let the “seed” wavefunction ψ^{flat} be the wavefunction for a massless scalar field in Minkowski spacetime with polynomial interactions (no derivatives) at time $t = 0$. In the next steps we derive the desired cosmological wavefunction by acting with a differential operator on ψ^{flat} . At tree-level, contributions to a wavefunction coefficient ψ_n^{flat} are represented by a tree diagram with V vertices, $I = V - 1$ edges (internal lines), and a number of external lines. The “bulk” representation of the corresponding wavefunction is given in terms of the following integral expression

$$\psi^{\text{flat}}(\{k_n\}; \{p_m\}) = i \int d^V t \left[\prod_{a=1}^n K(k_a) \right] \left[\prod_m^I G_{\text{flat}}(p_m) \right], \quad (3.1)$$

where the so-called *bulk-to-boundary propagator* $K(k, \eta)$ for a massless scalar in Minkowski is written in terms of the Minkowski mode functions ϕ_{flat}^+ as

$$K_{\text{flat}}(k, t) = \frac{\phi_{\text{flat}}^+(k, t)}{\phi_{\text{flat}}^+(k, 0)} = \frac{\frac{1}{\sqrt{2k}} e^{ikt}}{\frac{1}{\sqrt{2k}} e^{ik0}} = e^{ikt}. \quad (3.2)$$

⁹The results of [3] also apply to loop-level integrands, but we restrict our analysis to tree level.

The so-called *bulk-to-bulk propagator* G_{flat} contains a term proportional to the usual Feynman propagator but also an additional term that ensures the vanishing of G_{flat} as $t, t' \rightarrow 0$. It is explicitly given by

$$\begin{aligned} G_{\text{flat}}(t, t', k) &= iP_{\text{flat}}(k) [\theta(t-t')K_{\text{flat}}^*(t)K_{\text{flat}}(t') + \theta(t'-t)K_{\text{flat}}^*(t')K_{\text{flat}}(t) - K_{\text{flat}}(t)K_{\text{flat}}(t')] \\ &= i \left[\theta(t-t')\phi_{\text{flat}}^-(t)\phi_{\text{flat}}^+(t') + \theta(t'-t)\phi_{\text{flat}}^-(t')\phi_{\text{flat}}^+(t) - \phi_{\text{flat}}^+(t)\phi_{\text{flat}}^+(t') \frac{\phi_{\text{flat}}^-(t_0)}{\phi_{\text{flat}}^+(t_0)} \right], \\ &= \frac{i}{2k} \left[e^{-ik(t-t')}\theta(t-t') + e^{-ik(t'-t)}\theta(t'-t) - e^{ik(t+t')} \right]. \end{aligned} \quad (3.3)$$

Since K takes such a simple form, the integral representation of the wavefunction can also be written as

$$\psi^{\text{flat}}(\{k_n\}, \{p_m\}) = i \int d^V t e^{iq \cdot t} \prod_m^I G_{\text{flat}}(p_m), \quad (3.4)$$

where dot products of momenta and conformal time are taken to mean

$$q \cdot t = \sum_{A=1}^V q_A t_A, \quad (3.5)$$

and q_A is the sum of all external energies ending on the A vertex, $q_A = \sum k_a$ for $a \in A$. Note that the dependence of ψ^{flat} on the boundary energies k_n is only through the vertex energies q_A at each vertex. Because of this, in Steps 1 and Step 2 we do not need to know how many external lines are connected to a vertex, only the sum of those external energies appears.

The exchange energies p_m are uniquely fixed by imposing *momentum* conservation at every vertex. Notice however that “energy”, i.e. the norm $k = |\mathbf{k}|$ of the three-vectors \mathbf{k} is not conserved.

The seed functions ψ_n^{flat} can of course be computed explicitly expanding the products of bulk-to-bulk propagators and computing the time integrals in (4.4), but there are more efficient methods as described in [3]. Here we review the presentation in [3] of the Old-Fashioned Perturbation Theory (OFPT) expansion.

Consider

$$\left(\sum_A q_A \right) \psi^{\text{flat}} = i \int d^V \eta (\Delta_\eta e^{iq \cdot \eta}) \prod_m G_{\text{flat}}(p_m), \quad (3.6)$$

where we have inserted the time translation generator

$$\Delta_\eta = -i \sum_a \partial_{\eta_a}$$

We can integrate by parts to obtain

$$\left(\sum_A q_A \right) \psi^{\text{flat}} = -i \int d^V \eta e^{iq \cdot \eta} \sum_m \Delta_\eta G_{\text{flat}}(\eta_m, \eta'_m, p_m) \prod_{m' \neq m} G_{\text{flat}}(\eta_{m'}, \eta'_{m'}, p_{m'}) \quad (3.7)$$

We note that the time-ordered part of the propagator G_{flat} is time-translation invariant and therefore annihilated by Δ_η so that

$$\Delta_\eta G_{\text{flat}}(\eta_m, \eta'_m, p_m) = -i e^{ip_m(\eta_m + \eta'_m)}. \quad (3.8)$$

This has the effect of deleting the propagator and shifting the energies at the two relevant vertices. From this we derive the expression

$$\left(\sum_A q_A\right) \psi = \sum_m \psi_L^{+p_m} \text{---} m \text{---} \psi_R^{+p_m} + \psi_{l-1}^{+p_m} \text{---} m \text{---} \psi_{l-1}^{+p_m}, \quad (3.9)$$

where the sum runs over all deletions of a single edge m . We can ignore the term colored in red since we have restricted our analysis to tree level. The relevant term is therefore the first graphic corresponding to edges that disconnect the diagram upon deletion. The vertices connected by the deleted edge now absorb positive edge energy. This is made clear in (3.8). From the contact seed which is simply $1/p$ we can apply this recursive expression to efficiently build any seed function ψ^{flat} defined by the truncated diagram with associated edge and vertex energies. As discussed in [28], the algebraic nature of the above recursion relations can be traced back to the fact that in time-translation invariant theories the Schrödinger equation becomes algebraic.

3.1 Examples

Here we illustrate the recursive calculation of ψ^{flat} in Step 1 with some examples.

Two-site chain First we note that the base case is

$$\psi_1^{\text{flat}} = \bullet_q = \frac{1}{q}, \quad (3.10)$$

where q represents the sum of all the energies of the external legs attached to this vertex. Since it is only this sum that appears in all expression, when representing a diagram we don't show the external legs. For this contact interaction the diagram reduces to a single dot. Now we can consider the single factorization channel determining the two-site chain with intermediate energy p

$$(q_1 + q_2) \bullet \text{---} p \text{---} \bullet = \bullet_{q_1}^{+p} \mid \frac{+p}{q_2} \bullet. \quad (3.11)$$

This tells us that the wavefunction coefficient is

$$\psi_2^{\text{flat}} = \frac{\psi_1^{\text{flat}}(q_1 + p)\psi_1^{\text{flat}}(q_2 + p)}{q_T} = \frac{1}{(q_1 + q_2)(q_1 + p)(q_2 + p)}. \quad (3.12)$$

Three-site chain Now we move on to the three-site chain and comment on the general structure of the recursion graphically. Every term in the recursion is a sequence of cut edges and every cut corresponds to a product of contributions from the diagrams on either side of the cut. Every sequence terminates with all edges cut and therefore we get the inverse product of vertex energy q plus the energy of all edges landing on it, summed over all vertices. This motivates the circling depiction of contributions to the recursive sum.

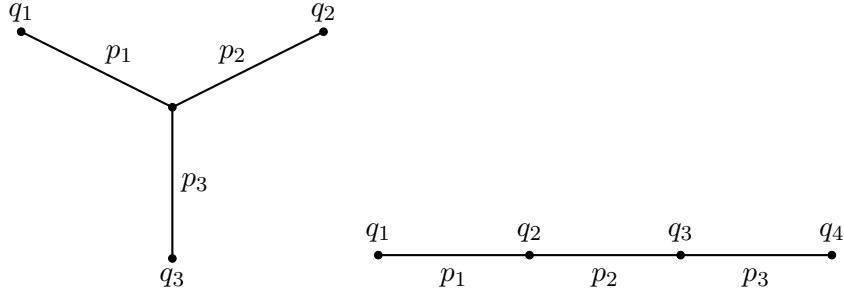


Figure 4: The two topologies for the four-site skeleton diagrams, namely the flux capacitor (left) and the four-site chain (right). The diagram also indicates the total external energies q_A associated with each vertex $A = 1, \dots, 4$ and the energy p_m of each internal line (edge) $m = 1, 2, 3$.

At each step we circle the two disconnected subgraphs produced by the deletion of a given edge. We then proceed within each subgraph until we reach individual vertices. Each circling furnishes a factor of the inverse of the sum of encircled vertex energies plus cut edge energies. Below we depict the two-site chain computed in the previous example:

$$\begin{array}{c} \text{---} \circ \text{---} \circ \text{---} \\ \text{---} p \text{---} \end{array} \quad \psi_2^{\text{flat}} = \frac{\psi_1^{\text{flat}}(q_1 + p)\psi_1^{\text{flat}}(q_2 + p)}{\sum_A^2 q_A} = \frac{1}{q_1 + q_2} \frac{1}{q_1 + p} \frac{1}{q_2 + p}. \quad (3.13)$$

Again, noting that each such contribution will contain the same total energy factor and individual vertex factors, which can be pulled out in front for any computation. Then what is left to be considered is all sequences of proper subgraphs with at least two vertices. We see this with the three-site chain.

$$\begin{array}{c} \text{---} \circ \text{---} \circ \text{---} \circ \text{---} \\ \text{---} p_1 \text{---} p_2 \text{---} \end{array} \quad (3.14)$$

$$\begin{aligned} \psi_3^{\text{flat}} &= \frac{\psi_2^{\text{flat}}(q_1, q_2 + p_2)\psi_1^{\text{flat}}(q_3 + p_2) + \psi_1^{\text{flat}}(q_1 + p_1)\psi_2^{\text{flat}}(q_2 + p_1, q_3)}{\sum_A^3 q_A} \\ &= \frac{1}{(q_1 + q_2 + q_3)(q_1 + p_1)(q_2 + p_1 + p_2)(q_3 + p_2)} \left(\frac{1}{q_1 + q_2 + p_2} + \frac{1}{q_2 + q_3 + p_1} \right), \quad (3.15) \end{aligned}$$

Where we depicted a sum over two choices of proper subgraph (equivalently, single edge deletions). The initial circling as well as the subsequent and complementary vertex circlings are omitted as their factors have been accounted for out front.

Four-site diagrams: the flux capacitor As a last example we discuss the two possible topologies for the four-site diagrams, namely the flux capacitor and the four-site chain. For the flux capacitor, with the kinematical assignments given in Figure 4, we find:

$$\psi_4^{\text{flat}} = \frac{\psi_3^{\text{flat}}(q_1, q_4 + p_3, q_2)\psi_1^{\text{flat}}(p_3 + q_3) + 2 \text{ perm's}}{q_1 + q_2 + q_3 + q_4} \quad (\text{flux capacitor}). \quad (3.16)$$

For the four-site chain, with kinematics given in Figure 4, we find the seed function

$$\psi_4^{\text{flat}} = \frac{1}{q_1 + q_2 + q_3 + q_4} \left[\psi_3^{\text{flat}}(q_1, q_2, q_3 + p_3) \psi_1^{\text{flat}}(p_3 + q_4) \right. \\ \left. + \psi_1^{\text{flat}}(q_1 + p_1) \psi_3^{\text{flat}}(p_1 + q_2, q_3, q_4) + \psi_2^{\text{flat}}(q_1, q_2 + p_2) \psi_2^{\text{flat}}(p_2 + q_3, q_4) \right] \quad (\text{four-site chain}). \quad (3.17)$$

The general procedure is straightforward, efficient, and readily furnishes the necessary seed functions with only algebraic manipulations.

4 Step 2: The intermediate wavefunction ψ_{int}

In this section, we prescribe differential operators that transform the flat spacetime wavefunction ψ^{flat} of Step 1 into an intermediate wavefunction, ψ_{int} , with the correct exchange propagators for a massless scalar field in dS up to overall powers of conformal time in the integrand. All the additional time dependence brought about from the vertices and the associate powers of spatial derivatives will be included in Step 3, which is discussed in the next section.

Before beginning the derivation let's briefly introduce our notation. For scalars, the bulk-to-boundary propagator K is given in terms of the mode functions ϕ^+ by

$$K(k, \eta) = \frac{\phi^+(k, \eta)}{\phi^+(k, 0)} = \frac{\frac{H}{\sqrt{2k^3}} (1 - ik\eta) e^{ik\eta}}{\frac{H}{\sqrt{2k^3}} (1 - ik0) e^{ik0}} = (1 - ik\eta) e^{ik\eta}, \quad (4.1)$$

where we took $\eta_0 \rightarrow 0$. The bulk-to-boundary propagator is

$$G(\eta, \eta', k) = iP(k) \left[\theta(\eta - \eta') K^*(\eta) K(\eta') + \theta(\eta' - \eta) K^*(\eta') K(\eta) - K(\eta) K(\eta') \right] \\ = i \left[\theta(t - t') \phi^-(t) \phi^+(t') + \theta(t' - t) \phi^-(t') \phi^+(t) - \phi^+(t) \phi^+(t') \frac{\phi^-(t_0)}{\phi^+(t_0)} \right], \quad (4.2)$$

where now the power spectrum for a canonically normalized massless scalar in de Sitter is $P(k) = H^2/(2k^3)$ and we set $H = 1$ throughout. Notice that $\partial_t K$ carries two powers of conformal time

$$\partial_t K(k, \eta) = \frac{1}{a} \partial_\eta K(k, \eta) = -Hk^2 \eta^2 e^{ik\eta}. \quad (4.3)$$

We denote derivatives with respect to t with a dot and those with respect to η with a prime. The above propagators and mode functions are invariant under the full dS isometries, including dS boosts. Conversely, we will allow for interactions that break dS boosts. This is important to capture many of the leading phenomenological models of inflation, where the breaking of dS boost is not slow-roll suppressed but can be large. In fact, for scalar perturbations in single-field inflation the breaking of boosts is a necessary condition to have non-vanishing connected correlators [14].

For simplicity, we will only consider parity even interactions, but we expect the generalization to the parity odd case to be straightforward. Assuming parity, every pair of spatial derivatives ∂_i needs to be contracted with the inverse metric $g^{ij} = \delta_{ij} \eta^2 H^2$, and so every spatial derivative carries one power of conformal time. The only inverse powers of conformal time come from $\sqrt{-g} = (H\eta)^{-4}$ in the measure of the covariant spacetime integral (in conformal time). For

example, a tree-level contribution to a de Sitter wavefunction coefficient ψ_n represented by a tree diagram with I internal lines and V vertices without any time derivatives takes the form

$$\psi(\{k_n\}; \{p_m\}; \{\mathbf{k}\}) = i \int \left[\prod_{A=1}^V d\eta_A F_A \prod_{a \in A} K(k_a, \eta_A) \right] \left[\prod_{m=1}^I G(p_m) \right], \quad (4.4)$$

where each conformal time η_A is integrated from $-\infty(1-i\epsilon)$ to 0 with $\epsilon > 0$ being taken to zero at the end of the calculation. This prescription projects out the Bunch-Davies vacuum in the past. Here, F_A represents the vertex factor associated to each vertex A and collects all contractions of spatial momenta and polarization tensors, as well as all the associated powers of η . Where no confusion arises, we will omit specifying the dependence of ψ_n on the internal energies p_m and the scalar products of momenta $\{\mathbf{k}\}$. In the presence of time derivative interactions some of the bulk-to-boundary propagators K may become K' and some of the bulk-to-bulk propagators $G = G_{\phi\phi}$ may become $G_{\phi'\phi}$, $G_{\phi\phi'}$ or $G_{\phi'\phi'}$.

4.1 Motivation

Before stating the general prescription for the intermediate wavefunction, we motivate it with an explicit example. Consider the time integral

$$\psi = i \int d\eta_1 d\eta_2 d\eta_3 e^{i \sum_A^3 q_A \eta_A} G_{\phi'\phi'}(\eta_1, \eta_2, p_1) G_{\phi'\phi}(\eta_2, \eta_3, p_2).$$

Using (2.10) and (2.11) and ignoring overall powers of conformal time we are motivated to consider the function

$$\psi_{\text{int}} = i \int d\eta_1 d\eta_2 d\eta_3 e^{i \sum_A^3 q_A \eta_A} [p_1^2 G_{\text{flat}}(\eta_1, \eta_2, p_1) - \delta(\eta_1 - \eta_2)] (1 - \eta_3 \partial_{\eta_3}) G_{\text{flat}}(\eta_2, \eta_3, p_2).$$

The quantities ψ_{int} and ψ differ by overall powers of the conformal times $\eta_{1,2,3}$. However, this difference can be fixed by taking an appropriate number of derivatives with respect to q_A , which act exclusively on the exponential bringing down the desired powers of $\eta_{1,2,3}$. This is something we will do in Step 3 and so, for the moment, we can neglect this difference. Our objective here is instead to express ψ_{int} as an operator acting on the three-site chain seed ψ_3^{flat} and the two-site chain seed ψ_2^{flat} (because of the δ -function term). Integrating by parts in η_3 , it is easy to see that the answer is

$$\psi_{\text{int}} = (2 + q_3 \partial_{q_3}) \left[p_1^2 \psi_3^{\text{flat}} - \psi_2^{\text{flat}} \right].$$

Via the application of external derivatives and contractions of polarization tensors and momenta, arbitrarily many external particles with arbitrary interactions can be attached to the three vertices. Therefore ψ_{int} corresponds to intermediate building block for infinite classes of wavefunction coefficients for massless scalars and gravitons. Let's now move on to consider arbitrary trees.

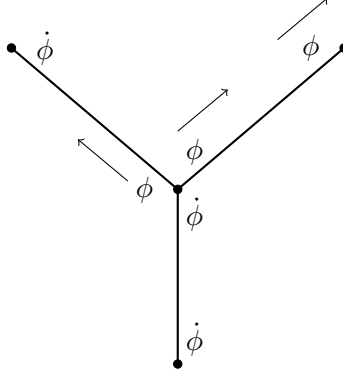


Figure 5: Edge-labeled diagram with a choice of routing for the two ϕ -type half-edges attached to the central vertex.

4.2 The general case

Recall the relations we found between derivatives of the de Sitter bulk-to-bulk propagator G and the flat space propagator G_{flat} , (2.9)-(2.11), which we report here for convenience

$$G_{\phi\phi}(\eta, \eta', p) = \frac{1}{p^2} [(1 - \eta\partial_\eta)(1 - \eta'\partial_{\eta'})G_{\text{flat}}(\eta, \eta', p) + \eta\eta'\delta(\eta - \eta')] , \quad (4.5)$$

$$G_{\phi'\phi'}(\eta, \eta', p) = \eta\eta' [p^2 G_{\text{flat}}(\eta, \eta', p) - \delta(\eta - \eta')] , \quad (4.6)$$

$$G_{\phi\phi'}(\eta, \eta', p) = (1 - \eta\partial_\eta)\eta' G_{\text{flat}}(\eta, \eta', p) = G_{\phi'\phi}(\eta', \eta, p) . \quad (4.7)$$

When all bulk-to-bulk propagators G for a given diagram have been re-written as above, we would like to interpret the resulting expression as a differential operator acting on a flatspace seed wavefunction ψ^{flat} . To do this, we have to overcome two obstacles. First we have to account for the factors $(1 - \eta\partial_\eta)$. We will now show that, by repeated use of integration by parts in time, we can trade these time derivatives for differential operators that act exclusively on external kinematics. We refer to this procedure as *re-routing*. Second, because of the delta functions appearing above, the corresponding term can be obtained by acting on a flatspace wavefunction ψ^{flat} with the relevant edge collapsed. In particular, for a generic diagram with a number $E_{\phi\phi}$ of $G_{\phi\phi}$ propagators and a number $E_{\phi'\phi'}$ of $G_{\phi'\phi'}$ propagators, we must sum over all combinations of collapsing $\langle\phi'\phi'\rangle$ and $\langle\phi\phi\rangle$ edges. This produces a sum over $2^{E_{\phi'\phi'} + E_{\phi\phi}}$ diagrams with only propagators and no δ -functions. We refer to this procedure as *collapsing*.

On re-routing Given a time integral with a factor of $(1 - \eta\partial_\eta)$ for every half-edge that is labeled by a ϕ , the objective is to re-route the time derivatives to a vertex that is connected only to a single exchange edge. Then a final integration by parts acts purely on external mode functions and can therefore be traded for a derivative with respect to some external energies q . To begin, we note the relation

$$(1 + p\partial_p - \eta_B\partial_{\eta_B} - \eta_A\partial_{\eta_A})G_{\text{flat}}(\eta_A, \eta_B, p) = 0 . \quad (4.8)$$

Given an edge that connects vertices at time η_A and η_B , consider the half-edge associated with time η_A . Using (4.8), we can choose to flow in one of two directions: either through the vertex

at time η_A or through the vertex at time η_B . This choice is depicted in Figure 2. In each case, integration by parts forces us to accumulate $(1 + p_m \partial_{p_m})$ for every edge m we flow through and $(1 + q_C \partial_{q_C})$ for every vertex C we flow through, with a relative sign between the two choices of direction. In this way we arrive at the following differential operators associated to each ϕ -type half-edge

$$\text{Re-routing vertex side:} \quad \Delta_{\text{rr}} = 1 + \left[\sum_C (1 + q_C \partial_{q_C}) + \sum_m (1 + p_m \partial_{p_m}) \right], \quad (4.9)$$

$$\text{Re-routing opposite-vertex side:} \quad \Delta_{\text{rr}} = 1 - \left[\sum_C (1 + q_C \partial_{q_C}) + \sum_m (1 + p_m \partial_{p_m}) \right], \quad (4.10)$$

where the sums run over all vertices¹⁰ C and edges m encountered as one flows from the given half-edge out of diagram. For each ϕ -type half edge, there are two choices for Δ_{rr} corresponding to flowing in the direction of the vertex to which the half-edge is attached, namely ‘‘vertex side’’, or in the opposite direction, namely ‘‘opposite vertex side’’. The rerouting procedure prescribed above relies upon the tree approximation.

On collapsing edges: To account for the delta functions in (4.5) and (4.6) we have to consider diagrams where one or more edges have been collapsed and the associated vertices have been merged. The re-routing operator in (4.9) is to be applied for each ϕ half-edge for each of the diagrams in the set of $2^{E_{\phi'} + E_{\phi}}$ ways of collapsing edges. We now provide some notation for organizing the collapsing of edges. It is important to distinguish between the the collapsing of $\phi\phi$ or $\phi'\phi'$ edges as they have a different factors. The differential operators we will discuss in Step 3 will act the sum of all collapsed contributions. Moreover, when both collapsing and re-routing are needed, the necessary re-routing operators Δ_{rr} need to be applied to each collapsed contribution. Here we specify what data is necessary to associate with the merged vertex produced upon collapsing an edge. Figure 6 depicts the two possibilities for collapsing. We consider an edge connecting vertices A and B collapsing down to an effective vertex AB . Denote as d_A and d_B the powers of conformal time at the respective vertices, which are given by (2.1). We find in each case

$$\text{collapsing } \phi\phi \rightarrow \eta_A^{d_A-4} \eta_B^{d_B-4} \left[\frac{1}{p^2} \eta_A \eta_B \delta(\eta_A - \eta_B) \right], \quad (4.11)$$

$$\text{collapsing } \phi'\phi' \rightarrow \eta_A^{d_A-4} \eta_B^{d_B-4} [-\delta(\eta_A - \eta_B)]. \quad (4.12)$$

Since the overall powers of η will be accounted for in Step 3, the factors that need to be included for each collapsed edge in Step 2 are simply

$$\text{collapsing } \phi\phi \rightarrow -\frac{1}{p^2} \partial_{q_A} \partial_{q_B} \quad \text{collapsing } \phi'\phi' \rightarrow -1. \quad (4.13)$$

¹⁰In our procedure *every* vertex C has some corresponding q_C , even if in the final graph there are no external legs attached to that vertex. This vertex energy q_C is hit by various ∂_{q_C} derivatives, as for example here in the re-routing operator or in (5.1) in Step 3. It is only *after* all derivatives have been taken that the q_C corresponding to a given vertex should be set to zero if there are no external lines attached to it.

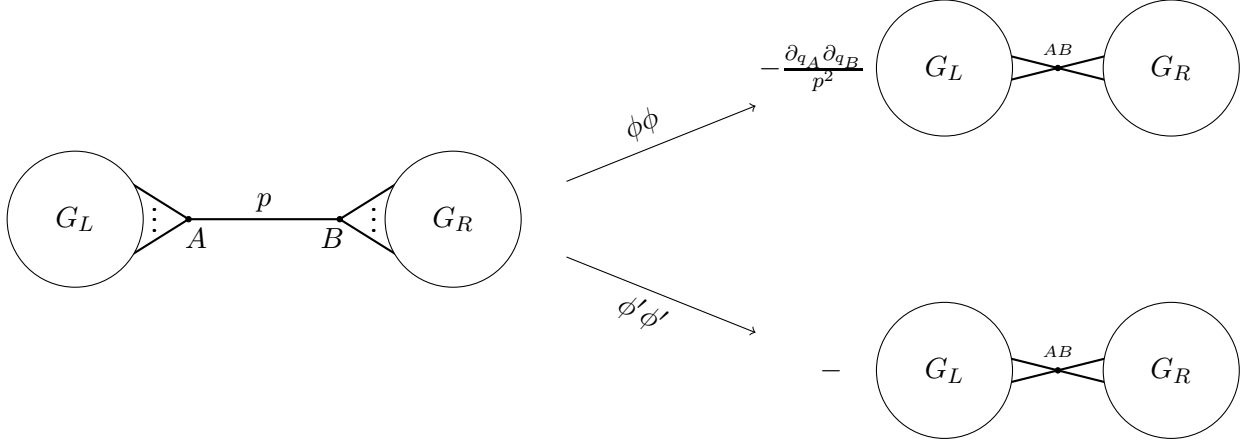


Figure 6: Here we depict edge collapsing in the case of $\phi\phi$ and $\phi'\phi'$ propagators. For $\phi\phi$ we need a factor of $p^{-2}\partial_{q_A}\partial_{q_B}$ whereas for $\phi'\phi'$ just a factor of -1 .

The above operators should be applied after the application of re-routing operators on the collapsed diagram. Finally, the overall powers of p_m in (4.5)-(4.7) require that we multiply all terms contributing in Step 2 by the overall factor

$$P = \prod_{\phi'\phi'} p_m^2 \prod_{\phi\phi} \frac{1}{p_m^2}, \quad (4.14)$$

where the products are over propagators of each type.

In summary, for each internal propagator in Step 2 we have to perform the following operations

$$\phi'\phi' \rightarrow \text{collapsing}, \quad \phi\phi' \rightarrow \text{re-routing}, \quad \phi\phi \rightarrow \text{collapsing \& re-routing}. \quad (4.15)$$

4.3 Examples

In the following we present several examples with two, three and four vertices (“sites”), respectively.

Two-site classification: Now we classify the different ψ_{int} with a two-site skeleton. There are three possibilities, corresponding to the three choices for the bulk-to-bulk propagator (up to permutations). The $\phi'\phi'$ case requires only collapsing an edge according to (4.12), but no re-routing. Since all overall factors of η will be included in Step 3, we can neglect them at this stage, and the result is simply

$$\begin{array}{c} \phi' \\ \bullet \\ q_1 \end{array} \xrightarrow{p} \begin{array}{c} \phi' \\ \bullet \\ q_2 \end{array} \quad \psi_{\text{int}}^{\phi'\phi'} = p^2 \psi_2^{\text{flat}}(q_1, q_2) - \psi_1^{\text{flat}}(q_1 + q_2), \quad (4.16)$$

where the arguments of ψ^{flat} refer to the sums q_1 and q_2 of external energies connected to each of the two vertices. For example, $\psi_{\text{flat},1}$ has a single external energy which should be taken to be the sum of the external energies at the two vertices that have been collapsed to one by the δ

function in (2.10). So it's argument is $q_1 + q_2$. Notice the factor of -1 in front of the contribution from collapsing the $\phi'\phi'$ edge, as dictated by (4.13).

The $\phi'\phi$ case requires re-routing with the operators in (4.9), but no collapsing is needed since there are no delta functions in (2.10). Re-routing the factor of $(1 - \eta'\partial_{\eta'})$ on the ϕ vertex side using the vertex-side operator in (4.9) we find

$$\begin{array}{c} \phi' \qquad \qquad \qquad \phi \\ \bullet \text{---} p \text{---} \bullet \\ q_1 \qquad \qquad \qquad q_2 \end{array} \quad \psi_{\text{int}}^{\phi'\phi} = (2 + q_2 \partial_{q_2}) \psi_2^{\text{flat}}(q_1, q_2). \quad (4.17)$$

The propagator $G_{\phi\phi}$ was given in (2.9). When re-written in terms of G_{flat} it has both a delta function and time derivatives so it needs both collapsing and re-routing (see (4.15)). Re-routing vertex-side each of the time derivatives with (4.9) we find the final result

$$\begin{array}{c} \phi \qquad \qquad \qquad \phi \\ \bullet \text{---} p \text{---} \bullet \\ q_1 \qquad \qquad \qquad q_2 \end{array} \quad \psi_{\text{int}}^{\phi\phi} = \frac{1}{p^2} (2 + q_1 \partial_{q_1}) (2 + q_2 \partial_{q_2}) \psi_2^{\text{flat}}(q_1, q_2) - \frac{1}{p^2} \partial_{q_1} \partial_{q_2} \psi_1^{\text{flat}}(q_1 + q_2). \quad (4.18)$$

These are the three ψ_{int} needed to compute the contribution to the exchange contributions to the trispectrum from $\dot{\phi}^3$ and $\dot{\phi}(\partial\phi)^2$ interactions. We begin to appreciate the advantages offered by our approach as we explore more complicated examples.

Three-site examples The next example is the three-site chain, namely a skeleton with two bulk-to-bulk propagators and three vertices. At tree level there is a single possible topology. By appropriately collapsing and re-routing we find

$$\begin{array}{c} \phi' \quad \phi' \quad \phi' \quad \phi' \\ \bullet \text{---} p_1 \text{---} \bullet \text{---} p_2 \text{---} \bullet \\ q_1 \quad \quad q_2 \quad \quad q_3 \end{array} = p_1^2 p_2^2 \psi_3^{\text{flat}} - p_1^2 \psi_{2L}^{\text{flat}} - p_2^2 \psi_{2R}^{\text{flat}} + \psi_1^{\text{flat}}, \quad (4.19)$$

$$\begin{array}{c} \phi \quad \phi' \quad \phi' \quad \phi' \\ \bullet \text{---} p_1 \text{---} \bullet \text{---} p_2 \text{---} \bullet \\ q_1 \quad \quad q_2 \quad \quad q_3 \end{array} = (2 + q_1 \partial_{q_1}) \left[p_2^2 \psi_3^{\text{flat}} - \psi_{2L}^{\text{flat}} \right],$$

$$\begin{array}{c} \phi \quad \phi \quad \phi' \quad \phi' \\ \bullet \text{---} p_1 \text{---} \bullet \text{---} p_2 \text{---} \bullet \\ q_1 \quad \quad q_2 \quad \quad q_3 \end{array} = \frac{1}{p_1^2} \left[(2 + q_1 \partial_{q_1}) (-1 - q_1 \partial_{q_1} - p_1 \partial_{p_1}) \psi_3^{\text{flat}} - p_2^2 \partial_{q_1} \partial_{q_2} \psi_{2R}^{\text{flat}} \right. \\ \left. - (2 + q_1 \partial_{q_1}) (2 + q_2 \partial_{q_2} + q_3 \partial_{q_3}) \psi_{2L}^{\text{flat}} - \psi_1^{\text{flat}} \right],$$

as well as

$$\begin{array}{c} \phi \quad \phi' \quad \phi \quad \phi' \\ \bullet \text{---} p_1 \text{---} \bullet \text{---} p_2 \text{---} \bullet \\ q_1 \quad \quad q_2 \quad \quad q_3 \end{array} = (2 + q_1 \partial_{q_1}) (-1 - q_3 \partial_{q_3} - p_2 \partial_{p_2}) \psi_3^{\text{flat}},$$

$$\begin{array}{c} \phi \quad \phi' \quad \phi' \quad \phi \\ \bullet \text{---} p_1 \text{---} \bullet \text{---} p_2 \text{---} \bullet \\ q_1 \quad \quad q_2 \quad \quad q_3 \end{array} = (2 + q_1 \partial_{q_1}) (2 + q_3 \partial_{q_3}) \psi_3^{\text{flat}},$$

$$\begin{array}{c} \phi' \quad \phi \quad \phi \quad \phi' \\ \bullet \text{---} p_1 \text{---} \bullet \text{---} p_2 \text{---} \bullet \\ q_1 \quad \quad q_2 \quad \quad q_3 \end{array} = (-1 - p_1 \partial_{p_1} - q_1 \partial_{q_1}) (-1 - p_2 \partial_{p_2} - q_3 \partial_{q_3}) \psi_3^{\text{flat}},$$

and finally

$$\begin{array}{c} \phi & \phi & \phi & \phi' \\ \bullet & \bullet & \bullet & \bullet \\ q_1 & p_1 & q_2 & p_2 & q_3 \end{array} = \frac{(-1 - q_3 \partial_{q_3} - p_2 \partial_{p_2})}{p_1^2} \left[(2 + q_1 \partial_{q_1}) (-1 - q_1 \partial_{q_1} - p_1 \partial_{p_1}) \psi_3^{\text{flat}} + \right. \\ \left. - \partial_{q_1} \partial_{q_2} \psi_{2R}^{\text{flat}} \right], \quad (4.20)$$

$$\begin{array}{c} \phi & \phi' & \phi & \phi \\ \bullet & \bullet & \bullet & \bullet \\ q_1 & p_1 & q_2 & p_2 & q_3 \end{array} = \frac{(2 + q_1 \partial_{q_1})}{p_2^2} \left[(2 + q_3 \partial_{q_3}) (-1 - p_2 \partial_{p_2} - q_3 \partial_{q_3}) \psi_3^{\text{flat}} - \partial_{q_2} \partial_{q_3} \psi_{2L}^{\text{flat}} \right],$$

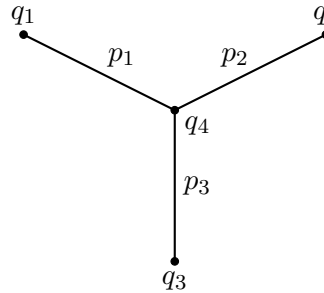
$$\begin{array}{c} \phi & \phi & \phi & \phi \\ \bullet & \bullet & \bullet & \bullet \\ q_1 & p_1 & q_2 & p_2 & q_3 \end{array} = \frac{1}{p_1^2 p_2^2} \left[(2 + q_1 \partial_{q_1}) (2 + q_3 \partial_{q_3}) (-1 - q_1 \partial_{q_1} - p_1 \partial_{p_1}) (-1 - q_3 \partial_{q_3} - p_2 \partial_{p_2}) \psi_3^{\text{flat}} - \right. \\ (2 + q_3 \partial_{q_3}) (-1 - q_3 \partial_{q_3} - p_2 \partial_{p_2}) \partial_{q_1} \partial_{q_2} \psi_{2R}^{\text{flat}} + \\ \left. - (2 + q_1 \partial_{q_1}) (-1 - q_1 \partial_{q_1} - p_1 \partial_{p_1}) \partial_{q_2} \partial_{q_3} \psi_{2L}^{\text{flat}} + \partial_{q_1} \partial_{q_2}^2 \partial_{q_3} \psi_1^{\text{flat}} \right]. \quad (4.21)$$

Notice that in each case there are $2^{E_{\phi'\phi} + E_{\phi\phi}}$ contributions, namely 1, 2 or 4, as expected on general grounds. Here we left the arguments of the seed wavefunction ψ^{flat} implicit, but they are recovered by the expressions below:

$$\psi_3^{\text{flat}} = \psi_3^{\text{flat}}(q_1, q_2, q_3; p_1, p_2), \quad \psi_{2R}^{\text{flat}} = \psi_2^{\text{flat}}(q_1 + q_2, q_3; p_2), \quad (4.22)$$

$$\psi_{2L}^{\text{flat}} = \psi_2^{\text{flat}}(q_1, q_2 + q_3; p_1), \quad \psi_1^{\text{flat}} = \psi_1^{\text{flat}}(q_1 + q_2 + q_3). \quad (4.23)$$

Four-site example: the flux capacitor As an example of a four-site chain with four vertices and three edges (bulk-to-bulk propagators), we study the flux capacitor with only ϕ'^n interactions, so that all half-edges are of the ϕ' type. Since all half-edges have one time derivative, all propagators are of the type $G_{\phi'\phi'}$ and we don't need any re-routing, only summing over all possible contractions. Using the following kinematical variables



$$\begin{array}{c} q_1 & & q_2 \\ & \swarrow p_1 & \searrow p_2 \\ & q_4 & \\ & \downarrow p_3 & \\ & q_3 & \end{array} \quad (4.24)$$

the result is

$$\begin{aligned} \psi_{\text{int}}^{\text{flux capacitor}} &= p_1^2 p_2^2 p_3^2 \psi_4^{\text{flat}}(q_1, q_2, q_3, q_4) - p_1^2 p_2^2 \psi_3^{\text{flat}}(q_1, q_4 + q_3, q_2) + 2 \text{ perm's} \\ &+ p_1^2 \psi_2^{\text{flat}}(q_1, q_2 + q_3 + q_4) + 2 \text{ perm's} - \psi_1^{\text{flat}}(q_1 + q_2 + q_3 + q_4). \end{aligned} \quad (4.25)$$

General ϕ'^n theory From the few examples above it is straightforward to see what ψ_{int} will be for a *general* tree diagram with only ϕ'^n interactions:

$$\psi_{\text{int}}^{\phi'^n} = \sum_{\text{collapsings}}^{2^I} \left[(-1)^{n_c} \psi_{n-n_c}^{\text{flat}} \prod_m^{I-n_c} p_m^2 \right]. \quad (4.26)$$

Here the sum is over the 2^I possible ways of collapsing any number n_c of the total I edges with a factor of (-1) for each of the collapsed edges and a factor of p_m^2 for each of the $I - n_c$ un-collapsed edges.

5 Step 3: The final de Sitter wavefunction ψ

In the last step, Step 3, we specify the interactions that take place at each of the vertices and determine the final operators we apply to obtain the desired de Sitter wavefunction.

The function ψ_{int} is dictated by the skeleton and number of time-derivatives on half-edges. From this point we can specify at each vertex an arbitrary $SO(3)$ invariant interaction which produces enough powers of conformal time to obey the bound in (2.1). Because we start from the function ψ^{flat} , which does not have the measure factor $\sqrt{-g} = (\eta H)^{-4}$, it need be the case that each vertex carries four or more powers of conformal time. In the next section we will discuss a generalisation to couplings in general relativity (GR), some of which have negative powers of η . Therefore, to get the correct result for a given interaction, we need to count the powers in excess of η^4 and produce them with derivatives acting on external energies. This net power of conformal time η_A at a given vertex is $d_A - 4$, where d_A (see (2.1)) is twice the number of time derivatives (since $\dot{K} \sim \eta K' \sim \eta^2$) plus the number of spatial derivatives (since $\partial_i \partial_j g^{ij} \sim \eta^2$). The minus four comes from the $\sqrt{-g} \sim \eta^{-4}$ measure of the spacetime integral. Therefore, we need to generate $d_A - 4$ additional powers of η_A with derivatives with respect to external kinematics¹¹ q_A . Furthermore, we also need to account for the fact that the bulk-to-boundary propagators for external legs are those in (4.1), which differ from the flat space propagators in (3.2) by a factor of $(1 - ik\eta)$. This missing factor can be simply generated by the acting with the differential operator $(1 - k_b \partial_{q_A})$ where k_b is the energy of an external leg that is attached to a vertex A with total external energy q_A .

Given the above discussion, we are now in the position of specifying the differential operator that need to act on each vertex A :

$$\Delta_A = i^{4-d_A} \left(\prod_{a \in K'} k_a^2 \right) \left(\prod_{b \in K} (1 - k_b \partial_{q_A}) \right) \frac{\partial^{d_A-4}}{\partial q_A^{d_A-4}}. \quad (5.1)$$

Here the first product goes over all external energies k_a of external legs that have one time derivative (bulk-to-boundary propagator K'), while the second goes over all external energies k_b of external legs without any time derivatives (bulk-to-boundary propagator K). An operator Δ_A

¹¹Since q_A is the sum of the external energies k_a for the legs attached to the vertex A , we could alternatively take this derivative with respect to any of these k_a .

must be applied for each vertex A . Notice that we are assuming throughout that the external mode functions are all massless de Sitter mode functions as in (4.1). The counting of derivatives is based on the uncollapsed graph, as the intermediate wave-function accounted already for all effects of collapsing.

Additionally, we must account for all contractions of spatial momenta and possibly polarization tensors that are dictated by the nature of the interaction at each vertex. These are given by the contractions of spatial vectors dictated by the spatial derivatives at each vertex. We denote this additional factor for all vertices collectively by F . In this way, we can express the final de Sitter wavefunction coefficient ψ as

$$\psi = F \left(\prod_A \Delta_A \right) \psi_{\text{int}}, \quad (5.2)$$

with the operator Δ_A defined in (5.1) and ψ_{int} the output of Step 2.

5.1 General properties

The tree-level contributions to wavefunction coefficients possess general properties that become manifest in our differential representation. We highlight some of these properties below.

Scale invariance Because of scale invariance, all contributions to the dS n -point wavefunction coefficient ψ_n must¹² scale as k^3 . This can be seen in the differential representation as follows. First notice that for a diagram with V vertices the flat spacetime seed function scales as

$$\psi_V^{\text{flat}} \sim k^{1-2V}. \quad (5.3)$$

Then, it's easiest to account in one go for both Step 2 and the factor of k^2 in Step 3 corresponding to a time derivative on an external leg. This can be thought of as a k for every ϕ' half-edge or ϕ' external leg, a k^{-1} for every ϕ half-edge, and a factor of k for every external leg. This correctly accounts for both the P factor in (4.14) and for the two prefactors in (5.1). Finally, the derivative in (5.1) gives a k^{4-d} for every vertex. Putting it all together we have

$$\frac{\partial \ln \psi_n}{\partial \ln k} \sim 1 - 2V + n + \sum_A^V (n_{\partial_i} + n_{\partial_t} - n_\phi) + \sum_B^V (4 - d_B) \quad (5.4)$$

$$\sim 1 - 2V + n + \sum_A^V (n_{\partial_i} + n_{\partial_t} - n_\phi + 4 - 2n_{\partial_t} - n_{\partial_i}) \quad (5.5)$$

$$\sim 1 - 2V + n + 4V - \sum_A n_A \quad (5.6)$$

$$\sim 1 + 2V + n - (2I + n) = 1 + 2(V - I) = 3, \quad (5.7)$$

¹²This scaling is violated by logarithmic corrections, which appear already at tree-level. The variation of logarithmic terms are analytical in two or more momenta (not energies) and therefore correspond to contact terms in position space. This mirrors the structure of Weyl anomalies in CFT's, as expected from AdS/CFT [51].

where n_ϕ is the number of fields *without time derivatives* in a given vertex A , such that $n_A = n_\phi + n_{\partial_t}$ is the valency of that vertex¹³. Also, in the fourth and fifth steps we used the graph identities

$$\sum_A n_A = 2I + n, \quad V = I + 1. \quad (5.8)$$

Partial and total energy poles The differential representation makes it clear that, by construction, the result is a rational function¹⁴. The only allowed poles are those that already exist in the seed wavefunction ψ^{flat} . The poles in ψ^{flat} are constrained to be very specific linear combinations of energy variables determined by the following construction [3]. Consider a general “skeleton” diagram, namely a diagram where all external legs have been removed. As always we associate an energy q_A to each vertex and an energy p_m to each edge. Let γ be a generic *connected* sub-diagram and let $\partial\gamma$ be the set of all edges that are (i) attached to vertices in γ and (ii) *not* included in γ . The corresponding partial energy variable is defined by

$$E_\gamma \equiv \sum_\gamma q_A + \sum_{m \in \partial\gamma} p_m. \quad (5.9)$$

The only possible poles in ψ_V^{flat} and hence in the full ψ_n are partial energies of some connected sub-diagram. This includes as a limiting case the total energy $k_T = \sum q_A = \sum_a k_a$ corresponding to the sub-diagram in question being the full diagram itself. Despite appearances, the factor p_m^{-2} in (4.14) does not introduce poles in the edge energies p_m because these are canceled by zeros in the associated bulk-to-bulk propagators. In fact, the absence of these divergences can be used as a starting point to derive the manifestly local test, as shown in [18].

Order of the total and partial energy poles The order of the total and partial energy poles are fixed by the mass dimensions of the vertices involved in the corresponding diagram. In general, if

$$\lim_{E_\gamma \rightarrow 0} \psi_n \sim \frac{1}{E_\gamma^{\text{p}_\gamma}} \quad (5.10)$$

we call¹⁵ p_γ the *order* of the corresponding partial energy pole. This obeys the upper bound

$$\text{p}_\gamma \leq 1 + \sum_{A \in \gamma} (\text{dim}_A - 4). \quad (5.11)$$

where dim_A is the mass dimension of the vertex A , given by¹⁶

$$\text{dim}_A = n_\phi + 2n_{\partial_t} + n_{\partial_i}. \quad (5.12)$$

¹³To avoid the cumbersome notation $n_{\partial_t}^A$, n_ϕ^A etc. we have left implicit the dependence on A of n_ϕ , n_{∂_t} and n_{∂_i} .

¹⁴Indeed the differential representation discussed so far is valid when all interactions obey $d \geq 4$ in which case no logarithmic terms can arise.

¹⁵We use the non-italicised “p” to avoid confusion with the edge energy p .

¹⁶Since n_ϕ counts only the ϕ ’s without time derivatives, we need a factors of 2 in front of n_{∂_t} to count the ϕ ’s with one time derivative.

When p corresponds to the total energy k_T , this upper bound on the order of the corresponding pole was derived in [17] using scale invariance and dimensional analysis. When p corresponds to the order of a partial energy poles, a bound can be derived using the cosmological cutting rules [20], which fix all terms with partial energy divergences [18] using unitarity. Instead, here we derive this bound from our differential representation. The seed wavefunction has a simple pole in all partial energies. The order of this pole increases by one when it is hit by a differential operator in Step 2 and Step 3 of our construction. In Step 2 we need to apply the re-routing operator for every internal half-edge of the ϕ type. This operator involves at most one derivative and therefore can raise the order of the pole by at most one. Notice that one can always choose the re-routing such that the half-edges external to a given sub-diagram never flows through that sub-diagram. Hence we need to only sum over the half-edges contained in a given sub-diagram. We can also increase the partial energy pole by one with the derivative term $k_b \partial_{q_A}$ in (5.1) for every external leg of the ϕ type. Finally, the ∂_{q_A} operators in (5.1) can increase the order by $d_A - 4$. Putting it all together we find

$$p_\gamma \leq 1 + \sum_A n_\phi^{\text{internal}} + \sum_B n_\phi^{\text{external}} + \sum_C (d_C - 4) \quad (5.13)$$

$$= 1 + \sum_A (n_\phi + n_{\partial_t} + n_{\partial_1} - 4) = 1 + \sum_{A \in \gamma} (\dim_A - 4), \quad (5.14)$$

which proves our claim.

Manifestly local test A theory is said to be manifestly local when all interactions are products of a fields and a finite number of their derivatives at the same spacetime point. The tree-level wavefunction coefficients for manifestly local theories of massless scalars and gravitons in dS must obey the simple condition (see [18] for more details)

$$\partial_{k_a} \psi_n(k_1, \dots, k_a, \dots, k_n; \dots) \Big|_{k_a=0} = 0. \quad (5.15)$$

where in taking the derivative one should keep fixed all internal energies p_m , all the other external energies k_b with $b \neq a$ and all contractions of spatial momenta $\mathbf{k}_a \cdot \mathbf{k}_b$. In other words, there is no linear term in k_a when Taylor expanding ψ_n around $k_a = 0$. It is straightforward to see that our differential representation indeed satisfies this manifestly local test. From the form of Δ_A in (5.1) it is immediately clear that for all external legs with a time derivative $\psi_a \sim \mathcal{O}(k_a^2)$ as $k_a \rightarrow 0$, which therefore satisfies (5.15). For external legs without time derivatives we notice that

$$\partial_{k_a} \left[\prod_b (1 - k_b \partial_{q_A}) F \right]_{k_a=0} = \partial_{k_a} \left[\prod_b (1 - k_b \partial_{k_b}) F \right]_{k_a=0} \quad (5.16)$$

$$= \left[- \prod_{b \neq a} (1 - k_b \partial_{k_b}) \partial_{k_a} F + \prod_b (1 - k_b \partial_{k_b}) \partial_{k_a} F \right]_{k_a=0} = 0. \quad (5.17)$$

5.2 Examples

To clarify our whole procedure we provide here the differential representations for a series of wavefunction coefficients.

One-site chain: contact diagrams As a natural starting point, we now compute contact diagrams. Even though these are quite easily computed also in the time-integral representation, they are simple enough to provide a good example of our procedure. For example consider the contact contribution to ψ_n from the interaction

$$\mathcal{L}_{\text{int}} = \frac{g}{n!} a^{4-n} (\phi')^n, \quad (5.18)$$

which has mass dimension $\text{dim} = 2n$. The flat space seed wavefunction of Step 1 is simply $\psi_1^{\text{flat}} = 1/q$ where q is the sum of all external energy and so can also be written as the more familiar total energy, $q = k_T$. Since there are no propagators, there is no need to perform Step 2. Finally, in Step 3 we hit ψ^{flat} with the operator in (5.1) where $d = 2n$:

$$\psi_n = g i^{2n-4} \left(\prod_a^n k_a \right)^2 \partial_{k_T}^{2n-4} \frac{1}{k_T} \quad (5.19)$$

$$= g i^{2n-4} (2n-4)! \frac{(\prod_a^n k_a)^2}{k_T^{2n-3}}. \quad (5.20)$$

We remind the reader that we work in units of the Hubble parameter, which is constant in de Sitter, so $H = 1$. Notice that the order p of the total energy pole $1/k_T^p$ matches what's expected on the general grounds of scale invariance and dimensional analysis [17]

$$p = 1 + \sum_A (\text{dim}_A - 4), \quad (5.21)$$

where in general the sum goes over all vertices A in the diagram. For the contact interaction in (5.18) this correctly reproduces $p = 2n - 3$, in agreement with (5.20).

As another example consider

$$\mathcal{L}_{\text{int}} = g a^{4-2n} (\partial_i \phi \partial_i \phi)^n, \quad (5.22)$$

which has mass dimension $\text{dim} = 4n$. The seed function of Step 1 is again $1/k_T$ and Step 2 is trivial. Finally, Step 3 gives us the final answer

$$\psi_{2n} = F i^{2n-4} \left[\prod_{a=1}^{2n} (1 - k_a \partial_{k_T}) \right] \partial_{k_T}^{2n-4} \frac{1}{k_T}, \quad (5.23)$$

where F is the sum over all permutations σ of the $2n$ external legs of the product of all possible pairings

$$F = \sum_{\sigma} (\mathbf{k}_{\sigma_1} \cdot \mathbf{k}_{\sigma_2}) (\mathbf{k}_{\sigma_3} \cdot \mathbf{k}_{\sigma_4}) \dots (\mathbf{k}_{\sigma_{2n-1}} \cdot \mathbf{k}_{\sigma_{2n}}). \quad (5.24)$$

The expression for ψ_{2n} can be re-written in terms of elementary symmetric polynomials e_a for

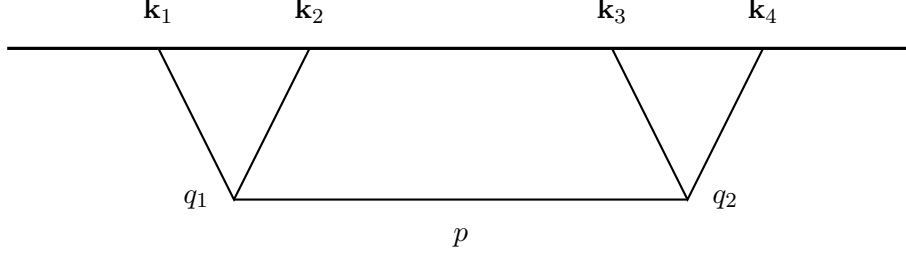


Figure 7: The scalar quartic wavefunction ψ_4^s from the exchange of the same scalar in the s -channel.

$2n$ variables

$$e_0 = 1, \quad (5.25)$$

$$e_1 = \sum_{1 \leq j_1 \leq 2n} k_{j_1} = k_T, \quad (5.26)$$

$$e_2 = \sum_{1 \leq j_1 < j_2 \leq 2n} k_{j_1} k_{j_2}, \quad (5.27)$$

...

$$e_a = \sum_{1 \leq j_1 < j_2 < \dots < j_a \leq 2n} k_{j_1} k_{j_2} \dots k_{j_a}, \quad (5.28)$$

$$e_{2n} = k_1 k_2 \dots k_{2n}. \quad (5.29)$$

The final wavefunction coefficient then becomes

$$\psi_{2n} = F i^{2n-4} \sum_{a=0}^{2n} e_a \frac{(2n+a-4)!}{k_T^{2n+a-3}}, \quad (5.30)$$

for which the largest total energy pole $p = 4n - 3$ is in agreement with the general result in (5.21).

Two-site chain: single-exchange diagram A more potent example of our differential representation is the calculation of the most important wavefunction coefficients generated by the leading operators in the Effective Field Theory of inflation [46]. Here we will discuss the quartic exchange wavefunction ψ_4^s in the s -channel. Other channels are simply obtained by permutations. We will consider all the possible combinations of the cubic, shift-symmetric interactions

$$\mathcal{L}_{int} = \frac{g_1}{3!} a(\phi')^3 + \frac{g_2}{2} a\phi'(\partial_i\phi)^2. \quad (5.31)$$

These are expected to be the leading ones in the decoupling limit. Let's start with the exchange generated by two insertions of $(\phi')^3$. In Step 1 we write down the corresponding flat space wavefunction

$$\psi_2^{\text{flat}} = \frac{1}{(q_1 + q_2)(q_1 + p)(q_2 + p)}, \quad \psi_1^{\text{flat}} = \frac{1}{q_1 + q_2}, \quad (5.32)$$

where the single vertex wavefunction $\psi_{\text{flat},1}$ will be needed in the contractions of the $\langle\phi'\phi'\rangle$ propagator. As depicted in Figure 7, we have two external legs attached to each vertex, so we have the relations

$$q_1 = k_1 + k_2, \quad q_2 = k_3 + k_4, \quad p = |\mathbf{k}_1 + \mathbf{k}_2|. \quad (5.33)$$

Moving on to Step 2, we can use the result of (4.16) to write

$$\psi_{\text{int}}^{\phi'\phi'} = p^2 \psi_2^{\text{flat}} - \psi_1^{\text{flat}} \quad (5.34)$$

$$= \frac{p^2}{(q_1 + q_2)(q_1 + p)(q_2 + p)} - \frac{1}{q_1 + q_2}. \quad (5.35)$$

Finally, moving on to Step 3, we have to apply one differential operator Δ_1 to the first vertex with the power of conformal time given by $d_1 = 2 \times 3 + 0 = 6$ and another Δ_2 to the other vertex with $d_2 = 6$. Hence, we find our final differential representation for this wavefunction coefficient:

$$\psi_4^{g_1 g_1} = g_1^2 (k_1^2 k_2^2 k_3^2 k_4^2) \partial_{q_1}^2 \partial_{q_2}^2 \psi_{\text{int}}^{\phi'\phi'}. \quad (5.36)$$

This is a very compact representation of the result and the derivatives can be calculated in a software such as Mathematica in a fraction of a second. The result is conveniently written in terms of $k_T = \sum_a k_a$, $E_L = q_1 + p$ and $E_R = q_2 + p$ in the form

$$\begin{aligned} \psi_4^{g_1 g_1} = 4g_1^2 (k_1 k_2 k_3 k_4 p)^2 & \left[\frac{6}{k_T^5 E_L E_R} + \frac{3}{k_T^4 E_L E_R} \left(\frac{1}{E_L} + \frac{1}{E_R} \right) + \frac{1}{k_T^3 E_L E_R} \left(\frac{1}{E_L} + \frac{1}{E_R} \right)^2 + \right. \\ & \left. + \frac{1}{k_T^2 E_L^2 E_R^2} \left(\frac{1}{E_L} + \frac{1}{E_R} \right) + \frac{1}{k_T E_L^3 E_R^3} - \frac{6}{p^2 k_T^5} \right]. \end{aligned} \quad (5.37)$$

As a second case we consider inserting the $(\phi')^3$ interaction on the left vertex, corresponding to q_1 and $\phi'(\partial_i \phi)^2$ on the other vertex, corresponding to q_2 . Step 1 is just the same as in the previous case and gives the flat space wavefunctions in (5.32). In Step 2 we encounter two types of propagators, the one corresponding to $\langle\phi'\phi'\rangle$, which we computed in (5.34), and the one corresponding to $\langle\phi'\phi\rangle$, which arises when the time derivative in $\phi'(\partial_i \phi)^2$ hits an external leg. For this latter case we can use (4.17)

$$\psi_{\text{int}}^{\phi'\phi} = (2 + q_2 \partial_{q_2}) \psi_2^{\text{flat}} \quad (5.38)$$

$$= \frac{q_1 q_2 + p(2q_1 + q_2)}{(p + q_1)(p + q_2)^2 (q_1 + q_2)^2}. \quad (5.39)$$

We are finally ready to perform Step 3 by acting with the differential operator in (5.1) on the two vertices, which have respectively $d_1 = 2 \times 3 + 0 = 6$ and $d_2 = 2 \times 1 + 2 = 4$. Accounting for the two possible propagators and the factor of F from the contraction of spatial derivatives on the second vertex, we find

$$\begin{aligned} \psi_4^{g_1 g_2} = -g_1 g_2 k_1^2 k_2^2 \partial_{q_1}^2 & \left\{ \mathbf{k}_3 \cdot \mathbf{k}_4 (1 - k_3 \partial_{q_2}) (1 - k_4 \partial_{q_2}) \psi_{\text{int}}^{\phi'\phi'} + \right. \\ & \left. + [\mathbf{k}_4 \cdot \mathbf{p} k_3^2 (1 - k_4 \partial_{q_2}) + \mathbf{k}_3 \cdot \mathbf{p} k_4^2 (1 - k_3 \partial_{q_2})] \psi_{\text{int}}^{\phi'\phi} \right\} \end{aligned} \quad (5.40)$$

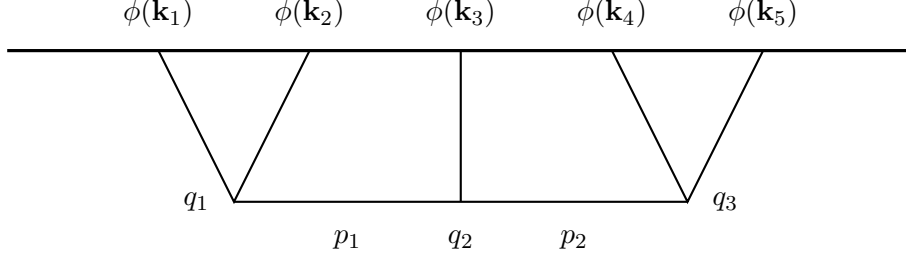


Figure 8: The scalar quintic wavefunction ψ_5^S from the double exchange of the same scalar.

As our last example, we derive the differential representation for two insertions of $\phi'(\partial_i\phi)^2$. This is the longest expression because it involves also a third type of exchange propagator without any time derivatives. The intermediate wavefunction for that case was worked out in Section 4.3. Following the prescribed rules, the full wavefunction is

$$\begin{aligned}
\psi_4^{g_2 g_2} = & g_2^2 [(\mathbf{k}_1 \cdot \mathbf{k}_2)(\mathbf{k}_3 \cdot \mathbf{k}_4)(1 - k_1 \partial_{q_1})(1 - k_2 \partial_{q_1})(1 - k_3 \partial_{q_2})(1 - k_4 \partial_{q_2})\psi_{\text{int}}^{\phi' \phi'} \\
& + k_3^2(\mathbf{k}_1 \cdot \mathbf{k}_2)(\mathbf{p} \cdot \mathbf{k}_4)(1 - k_1 \partial_{q_1})(1 - k_2 \partial_{q_1})(1 - k_4 \partial_{q_2})\psi_{\text{int}}^{\phi' \phi} \\
& + k_2^2(\mathbf{k}_1 \cdot \mathbf{p})(\mathbf{k}_3 \cdot \mathbf{k}_4)(1 - k_1 \partial_{q_1})(1 - k_3 \partial_{q_2})(1 - k_4 \partial_{q_2})\psi_{\text{int}}^{\phi' \phi} + \\
& k_1^2 k_3^2(\mathbf{k}_2 \cdot \mathbf{p})(\mathbf{k}_4 \cdot \mathbf{p})(1 - k_2 \partial_{q_1})(1 - k_4 \partial_{q_2})\psi_{\text{int}}^{\phi \phi}] + 3 \text{ perms}, \quad (5.41)
\end{aligned}$$

where it's understood that in each exchange class we sum over the necessary permutations of labels for external lines and the three ψ_{int} are given in (4.16), (4.17) and (4.18). Here the three permutations correspond the exchange of $1 \leftrightarrow 2$, $3 \leftrightarrow 4$ and the combination of these two.

Three-site chain: double-exchange diagram The previous examples discussed diagrams for which the integral bulk representation is still a practical computational tool because there are at most two nested time integrals. Here we want to show that the differential representation remains quite simple and easy to derive also when the number of nested time integrals grows, which makes a brute force bulk time integration very slow. As an example, we discuss the (tree-level) five-point function from three insertions of $(\phi')^3$. For Step 1 we need the flat space wavefunction corresponding to the three site chain, which we computed in (3.14) (see Figure 8 for the definition of kinematical variables)

$$\psi_3^{\text{flat}} = \frac{1}{(q_1 + q_2 + q_3)(q_1 + p_1)(q_2 + p_1 + p_2)(q_3 + p_2)} \left(\frac{1}{q_1 + q_2 + p_2} + \frac{1}{q_2 + q_3 + p_1} \right). \quad (5.42)$$

The corresponding intermediate wavefunction was computed in (4.19),

$$\psi_{\text{int}}^{\phi' \phi' \phi' \phi'} = p_1^2 p_2^2 \psi_3^{\text{flat}} - p_1^2 \psi_{2L}^{\text{flat}} - p_2^2 \psi_{2R}^{\text{flat}} + \psi_1^{\text{flat}}, \quad (5.43)$$

where ψ_{2L}^{flat} is the flat space wave-function for a two-site chain for the diagram made from collapsing the p_2 exchange edge and ψ_{2R}^{flat} is that made from collapsing the p_1 exchange edge. Since the ϕ'^3

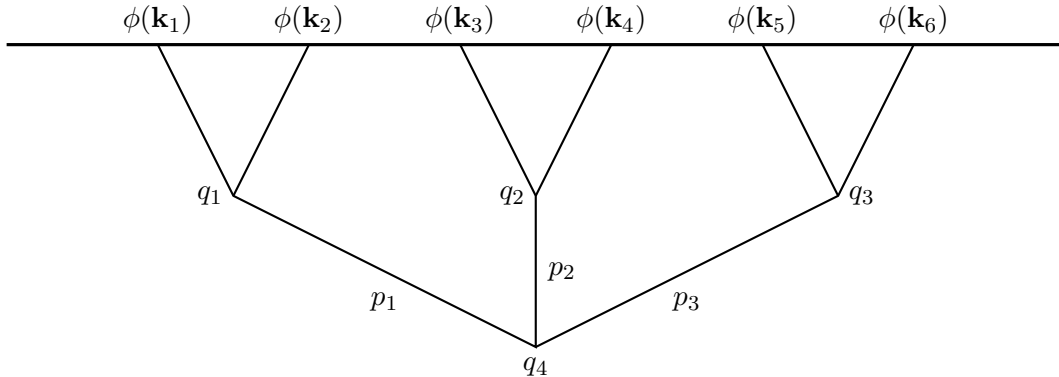


Figure 9: The flux capacitor contribution to the 6-point function ψ_6 from the interaction $\phi^3/3!$

interaction has $d = 6$, the desired de Sitter wavefunction is simply

$$\psi_5^{g_1^3} = - \left(\prod_{a=1}^5 k_a^2 \right) \partial_{q_1}^2 \partial_{q_2}^2 \partial_{q_3}^2 \psi_{\text{int}}^{\phi' \phi' \phi' \phi'}. \quad (5.44)$$

Four-site chain: the flux capacitor Using the result for the flux-capacitor intermediate wavefunction ψ_{int} in (4.25), and assuming that all interactions are of the form $\phi^3/3!$, it is immediate to write down the six-point wavefunction coefficient associated with the diagram in Figure 9

$$\psi_6 = \prod_{a=1}^6 k_a^2 \prod_{A=1}^4 \partial_{q_A}^2 \psi_{\text{int}}. \quad (5.45)$$

General ϕ'^n theory For a general theory with ϕ'^n interactions for any set of n 's, we computed the intermediate wavefunction in (4.26) for any tree-level diagram with an arbitrary number of internal and external propagators. Using that fact that a ϕ'^n interaction has $d = 2n$, we find that the final dS wavefunction is simply given by

$$\psi_n = \prod_{a=1}^n k_a^2 \prod_{A=1}^V (-1)^{n_A} \partial_{q_A}^{2n_A-4} \psi_{\text{int}}, \quad (5.46)$$

where n_A is the valency of the vertex A and ψ_{int} was given in (4.26).

6 Minimal coupling to gravity

In this section, we show how to generalise our differential representation to describe gravitational interactions, which contain terms with only two spatial derivatives and hence violate the inequality in (2.1). This issue can be overcome both for contact and exchange diagrams at tree level. As concrete examples, we discuss the quartic scalar and quartic graviton wavefunction coefficients induced by graviton exchange in GR.

6.1 Contact diagrams

To describe minimal coupling to gravity, we need to accommodate interactions with two derivatives. Two time derivatives are already accounted for by our previous treatment because they satisfy (2.1). Assuming parity, the only other option¹⁷ is an interaction with two spatial derivatives. Since this has $d = 2$ it violates (2.1) and has the following time-dependent integrand (up to overall factors of \mathbf{k})

$$i \int d\eta a^2 K^n, \quad (6.1)$$

with K the massless propagators in (4.1). At the contact level, this interaction does not yield a finite wavefunction as it has a divergent imaginary part. This can be seen by counting the powers of η . However, notice that, for parity-even interactions, it is only the real part of ψ that contributes to the correlator. This is IR finite despite the $1/\eta$ divergence in the imaginary part of ψ . Explicitly, the n -point contact diagram produces the integral

$$\psi_c = i \int \frac{d\eta}{\eta^2} \prod_{a=1}^n (1 - ik_a \eta) e^{ik_a \eta}. \quad (6.2)$$

How can we obtain this $1/\eta^2$ term by acting with derivatives on the flat-space seed wavefunction, where no such factor is present? We observe that the above can be re-expressed as

$$\psi_c = i \int d\eta \left[-\partial_\eta \left(\frac{e^{ik_T \eta}}{\eta} \right) - \sum_{p=2}^n (-i\eta)^{p-2} e_p(\{k_a\}) e^{ik_T \eta} \right], \quad (6.3)$$

where $e_p(\{k_a\})$ is the elementary symmetric polynomial of order p in the k_a 's, e.g. $e_2(u, v, w) = uv + uw + vw$. The $\eta \rightarrow 0$ limit produces a divergence in the first term. If we consider the real part, the divergence drops out and we find

$$\text{Re } \psi_c = -\frac{i}{2} \lim_{\eta_0 \rightarrow 0} \frac{e^{ik_T \eta_0} - e^{-ik_T \eta_0}}{\eta_0} - \sum_{p=2}^n e_p(\{k_a\}) \frac{(p-2)!}{k_T^{p-1}}, \quad (6.4)$$

and so we have

$$\text{Re } \psi_c = k_T - \sum_{p=2}^n e_p(\{k_a\}) \frac{(p-2)!}{k_T^{p-1}}. \quad (6.5)$$

This is in agreement with the classic result in [31]. For more general diagrams we need to accommodate exchange diagrams containing vertices with $d = 2$, of the same form as 6.1. The total derivative leveraged in equation (6.3) allows us to do this.

¹⁷When solving for the constrained lapse and shift one also generates non-manifestly local interactions for the graviton and for gravitationally coupled scalars. Counting an inverse Laplacian as contributing -2 to n_{∂_i} , we have checked that these interactions all have $d \geq 4$ and so fall within the regime of applicability of the techniques we have presented in the first part of the paper, where manifest locality was not assumed.

6.2 Exchange Diagrams

In an exchange diagram, the vertex in (6.1), which has $d = 2$, will generically have l bulk-to-boundary propagators and $n - l$ bulk-to-bulk propagators attached to it:

$$\int \cdots \int \frac{d\eta}{\eta^2} \prod_{a=1}^l (1 - ik_a \eta) e^{ik_a \eta} \prod_{m=1}^{n-l} G(\eta, \eta'_m, p_m). \quad (6.6)$$

As in the contact case, we can express this as

$$\int \cdots \int d\eta \left[-\partial_\eta \left(\frac{e^{iq_A \eta}}{\eta} \right) - \sum_{p=2}^l (-i\eta)^{p-2} e_p(\{k_a\}) e^{iq_A \eta} \right] \prod_{m=1}^{n-l} G(\eta, \eta'_m, p_m), \quad (6.7)$$

where $q_A = \sum^l k_a$. We can integrate by parts and observe that

$$\lim_{\eta \rightarrow 0} \frac{1}{\eta} \prod_{i=1}^{n-l} G(\eta, \eta'_i, p_m) = 0, \quad (6.8)$$

which ensures the vanishing of the boundary term. Therefore the portion of the time-integral from this vertex is

$$\int \cdots \int d\eta e^{iq_A \eta} \left[\frac{1}{\eta} \partial_\eta - \sum_{p=2}^l (-i\eta)^{p-2} e_p(\{k_a\}) \right] \prod_{m=1}^{n-l} G(\eta, \eta'_m, p_m). \quad (6.9)$$

Applying this argument to diagrams with multiple vertices with $d = 2$ we end up with

$$\int \prod_A d\eta_A e^{iq_A \eta_A} \left[\frac{1}{\eta_A} \partial_{\eta_A} - \sum_{p=2}^l (-i\eta_A)^{p-2} e_p(\{k_a\}) \right] \prod_{m=1}^I G(p_m). \quad (6.10)$$

Thus far we have merely performed the same integration by parts employed in the contact case at all vertices in an exchange graph. In (6.10) this is expressed as an operator in conformal time acting on $G = G_{\phi\phi}$ propagators. That is, in the language of previous sections, we have time derivatives or powers of conformal time acting on half-edges of the ϕ type. Notice that when ∂_η acts on the propagator we get an additional factor of conformal time as in (2.10), so the expression in (6.10) manifestly satisfies the condition in (2.1) at the vertex in question. Indeed we see that the application of the derivative expands the time integral in (6.9) into a sum over $n - l + 1$ time integrals of the type computed in previous sections.

Generically, when the number of symmetric polynomial terms $l - p$ is greater than 1, we cannot write a “local” differential operator acting on the seed function (conversely this is possible for the leading $n = 3$ case which we consider below). The difference between these is the Δ_A operator, which accounts for the overall power of conformal time at the vertex A . However, these differing operators will not in general commute with the differential operators associated with other parts of the diagram and therefore cannot be locally lumped with the operator coming from $\frac{1}{\eta} \partial_\eta$. Therefore, for general n one must consider a sum of 2^{V_g} diagrams where V_g is the number of

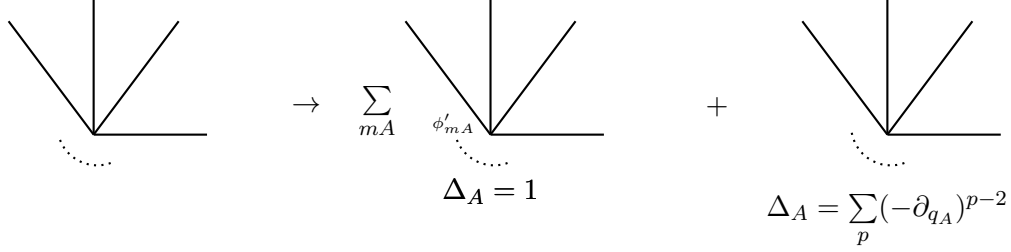


Figure 10: Expansion for vertices of type $\frac{1}{\eta^2} \prod (\phi_{ml})_i$ where ϕ_{ml} denotes massless mode function. The first term in the expansion denotes a sum over half-edges Am , namely the part of edge m ending on the vertex A , where that half-edge becomes a ϕ' . In the second term all half-edges are of the ϕ -type, corresponding to the ordinary massless mode functions.

vertices with $d = 2$. At each vertex we must apply the local expansion depicted in Fig. 10. The expansion has two terms: one for the time derivative portion of (6.9) and one for the second term. We can prescribe the associated differential operators for each of these. For the first diagram, coming from the time derivative term, we have differential operators:

$$\begin{cases} \Delta_{\text{grav}}^{\phi'} = \sum_{m=1}^{n-l} p_m \prod_{m' \neq m} \frac{1}{p_{m'}} \Delta_{\text{rr}}^{m'A}, \\ \Delta_A = 1, \end{cases} \quad (6.11)$$

where the sum runs over all $n - l$ bulk-to-bulk propagators that are hit by the time derivative, and the product is over the remaining propagators. The second term has differential operators

$$\begin{cases} \Delta_{\text{grav}}^{\phi} = \sum_{p=2} e_p(\{k_a\}) \prod_m \frac{1}{p_m} \Delta_{\text{rr}}^{mA}, \\ \Delta_A = - \sum_{p=2} (-\partial_{q_A})^{p-2}. \end{cases} \quad (6.12)$$

In these expressions we have specified where the re-routing operator Δ_{rr} starts from, namely from the half-edge mA which is the part of the edge m that ends on the vertex A . These operators completely prescribe the computation of the uncollapsed contribution, but we still have to specify the collapsed contribution.

The complete prescription requires specification of the complementary half-edges on each propagator. However, while remaining agnostic about A' we can restate the relevant form of equation 4.11 for a vertex A :

$$\text{collapsing } \phi\phi \rightarrow \left(\sum_p e_p(\{k_a\}) (-\partial_{q_A})^{p-2} \right) \eta_{A'}^{d_{A'}-4} \left[\frac{1}{p^2} \eta_A \eta_{A'} \delta(\eta_A - \eta_{A'}) \right], \quad (6.13)$$

$$\text{collapsing } \phi'\phi' \rightarrow \eta_{A'}^{d_{A'}-4} [-\delta(\eta_A - \eta_{A'})]. \quad (6.14)$$

n = 3 We now restrict to the case of $n = 3$ and provide some examples. This involves the by now familiar collapsing procedure, coming from the ϕ' or ϕ that has been generated via the respective term in the integration by part being paired with ϕ or ϕ' at A' . The leading gravitational interactions have $n = 3$. After integration by part, the vertex is

$$\int \dots \int d\eta e^{iq_A \eta} \left[\frac{1}{\eta} \partial_\eta - e_2(\{k_a\}) \delta_{l1} \right] \prod_{i=1}^l G(\eta, \eta'_i, p_m) \quad (6.15)$$

where the Kronecker δ_{l1} manifests that we only get the second term inside the square brackets if we have precisely one exchange propagator attached to the vertex in question. This case is particularly simple because of the absence of overall powers of η at this vertex that need be accounted for and we can prescribe the differential operator locally, without the generic expansion over multiple diagrams described above. In particular, the differential operator associated to a vertex is

$$\Delta_{\text{grav}}^A = \left[\sum_{m=1}^l p_m \prod_{m' \neq m} \frac{1}{p_{m'}} \Delta_{\text{rr}}^{m'A} \right] - e_2(\{k_a\}) \delta_{l1} \prod_m \frac{1}{p_m} \Delta_{\text{rr}}^{mA}, \quad (6.16)$$

where the sum and products over m and m' run only over the l internal lines. The differential operators Δ_{rr} starting from an half-edge mA were defined in (2.12) and depend on the energy variables in the diagram; it should be understood that these are defined on a common choice of energy flow out of the diagram as depicted in Figure 2. Moreover, the differential operator associated with this vertex at the final step is trivial, as all η dependence has been accounted for, $\Delta_A = 1$, leaving only tensor and momentum contractions to be multiplied out front. The final ingredient to be accounted for is the collapsing of edges. The collapsing proceeds in the same way as described previously. In all cases, the vertex in (6.15) implies $d_A = 4$, and the specific contractions depend on the vertices to which A is connected. Below we apply this prescription to four-point exchange diagrams. As an example, consider the following time integral:

$$I = \int d\eta_1 d\eta_2 e^{iq_1 \eta_1} e^{iq_2 \eta_2} \left[\eta_1^{-1} \partial_{\eta_1} - \frac{k_1 k_2}{p} \right] \left[\eta_2^{-1} \partial_{\eta_2} - \frac{k_3 k_4}{p} \right] G_{\phi\phi}(\eta_1, \eta_2, p) \quad (6.17)$$

This is the time integral relevant for graviton exchange in minimal coupling to gravity. We have applied the integration by part discussed above to both vertices. Note that the term with two time derivatives $\partial_{\eta_1} \partial_{\eta_2}$ and the term without any time derivative will correspond to $\phi' \phi'$ and $\phi \phi$ propagators respectively. These propagators display delta functions that need to be accounted for by the procedure of collapsing. In the next section we will use the differential operator prescription to compute the wavefunction for this process.

6.3 Example: Scalars exchanging a graviton

A massless scalar ϕ minimally coupled to gravity has the following interaction vertex with transverse-traceless tensor fluctuations γ_{ij} :

$$S_{\text{int}} = \int \frac{d\eta}{\eta^2} d^3 x \gamma^{ij} \partial_i \phi \partial_j \phi. \quad (6.18)$$

In the following we compute the contribution to the four-scalar wavefunction coefficient ψ_4

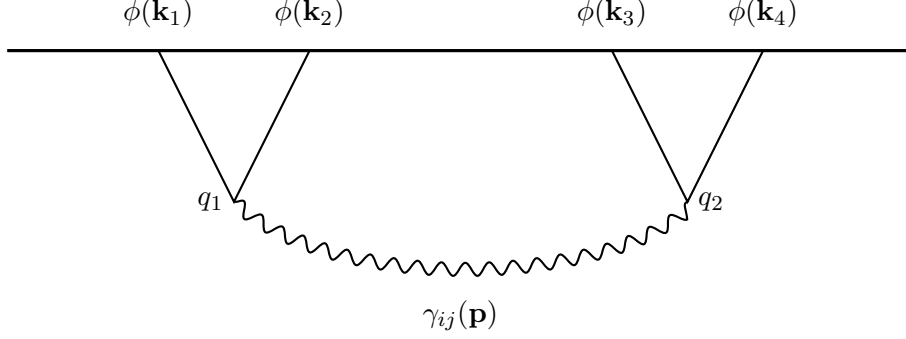


Figure 11: The s -channel graviton-exchange contribution to ψ_4 .

from the s -channel exchange of a graviton and two insertions of this interaction, as depicted in Figure 11. This was previously computed in [52] using the bulk representation and in [53] for the wavefunction (see also [15]). Let's use the above prescription for one of the two interaction vertices. We notice that each vertex has a single internal line attached, so we should choose $l = 1$ in (6.16). This implies that both terms in (6.16) are non-vanishing. The left vertex with $q_1 = k_1 + k_2$ energy gives the differential operator

$$\Delta_{\text{grav}}^{\text{Left}} = p - \frac{e_2(k_1, k_2)}{p}(2 + q_1 \partial_{q_1}) = p - \frac{k_1 k_2}{p}(2 + q_1 \partial_{q_1}), \quad (6.19)$$

where we have used the vertex-side definition of Δ_{rr} in (2.12). Combining the differential operators of each vertex one finds

$$\Delta_{\text{grav}} = \Delta_{\text{grav}}^{\text{Left}} \Delta_{\text{grav}}^{\text{Right}} \quad (6.20)$$

$$= \left[p - \frac{k_1 k_2}{p}(2 + q_1 \partial_{q_1}) \right] \left[p - \frac{k_3 k_4}{p}(2 + q_2 \partial_{q_2}) \right], \quad (6.21)$$

where we cut our momentum flow along the single internal line. This differential operator fully accounts for the exchanged time integral. We finally account for collapsed contributions, of which there are two: one of the $\langle \phi' \phi' \rangle$ type, corresponding to the term with two time derivatives in (6.17), and one of the $\langle \phi \phi \rangle$ type, corresponding to the term without any time derivatives. These contribute in the same way as discussed in Section 4, with two time derivatives needed on the $\langle \phi \phi \rangle$ collapse. Therefore we have

$$\text{collapsed contribution: } - \left(1 + \frac{k_1 k_2 k_3 k_4}{p^2} \partial_{q_1} \partial_{q_2} \right) \psi_1^{\text{flat}}, \quad (6.22)$$

where $\psi_1^{\text{flat}} = k_T^{-1}$ with $k_T = \sum k_a = q_1 + q_2$. Putting together all contributions we find

$$\psi_{4\phi} = F \left[- (1 + k_1 k_2 k_3 k_4 \partial_{q_1} \partial_{q_2}) \psi_1^{\text{flat}} + \Delta_{\text{grav}}^{\text{Left}} \Delta_{\text{grav}}^{\text{Right}} \psi_2^{\text{flat}} \right] \quad (6.23)$$

$$= F \left[- \frac{1}{k_T} - \frac{2k_1 k_2 k_3 k_4}{k_T^3 p_1^2} + \left(p_1 - \frac{k_1 k_2}{p_1}(2 + q_1 \partial_{q_1}) \right) \left(p_1 - \frac{k_3 k_4}{p_1}(2 + q_2 \partial_{q_2}) \right) \psi_1^{\text{flat}} \right], \quad (6.24)$$

where ψ^{flat} is the flatspace seed function in (3.12), and the vertex is given by

$$F = \sum_{s=\pm} \epsilon_{ij}^s(\mathbf{p}) \epsilon_{kl}^s(-\mathbf{p}) k_1^i k_2^j k_3^k k_4^l, \quad (6.25)$$

with \mathbf{p} the internal momentum $\mathbf{p} = \mathbf{k}_1 + \mathbf{k}_2$. This sum can be re-written without any reference to the polarization tensors $\epsilon_{ij}^s(\mathbf{p})$ using (see e.g. [4])

$$\sum_{s=\pm 2} = \epsilon_{ij}^s(\mathbf{p}) \epsilon_{kl}^s(-\mathbf{p}) = \pi_{ik} \pi_{jl} + \pi_{il} \pi_{jk} - \pi_{ij} \pi_{kl}, \quad \pi_{ij} \equiv \delta_{ij} - \frac{p_i p_j}{p^2}, \quad (6.26)$$

This gives

$$\epsilon_{ij}^s \epsilon_{kl}^s k_1^i k_2^j k_3^k k_4^l = \left(\mathbf{k}_1 \cdot \mathbf{k}_3 + \frac{\mathbf{k}_1 \cdot \mathbf{p} \mathbf{k}_3 \cdot \mathbf{p}}{p^2} \right) \left(\mathbf{k}_2 \cdot \mathbf{k}_4 + \frac{\mathbf{k}_2 \cdot \mathbf{p} \mathbf{k}_4 \cdot \mathbf{p}}{p^2} \right) \quad (6.27)$$

$$+ \left(\mathbf{k}_1 \cdot \mathbf{k}_4 + \frac{\mathbf{k}_1 \cdot \mathbf{p} \mathbf{k}_4 \cdot \mathbf{p}}{p^2} \right) \left(\mathbf{k}_2 \cdot \mathbf{k}_3 + \frac{\mathbf{k}_2 \cdot \mathbf{p} \mathbf{k}_3 \cdot \mathbf{p}}{p^2} \right) \quad (6.28)$$

$$- \left(\mathbf{k}_1 \cdot \mathbf{k}_2 + \frac{\mathbf{k}_1 \cdot \mathbf{p} \mathbf{k}_2 \cdot \mathbf{p}}{p^2} \right) \left(\mathbf{k}_3 \cdot \mathbf{k}_4 + \frac{\mathbf{k}_3 \cdot \mathbf{p} \mathbf{k}_4 \cdot \mathbf{p}}{p^2} \right). \quad (6.29)$$

6.4 Example: Gravitons exchanging a graviton

If we consider the tensor self-interaction at third order we have the vertex

$$\int \frac{d\eta}{\eta^2} d^3x \left(\gamma_{ik} \gamma_{jl} - \frac{1}{2} \gamma_{ij} \gamma_{kl} \right) \partial_k \partial_l \gamma_{ij}, \quad (6.30)$$

which produces an identical time integral as the one in the previous example but a different polarization structure out front. In particular one has

$$\psi_{4\gamma} = F \left[-\frac{1}{k_T} - \frac{2k_1 k_2 k_3 k_4}{k_T^3 p_1^2} + \left(p_1 - \frac{k_1 k_2}{p_1} (2 + q_1 \partial_{q_1}) \right) \left(p_1 - \frac{k_3 k_4}{p_1} (2 + q_2 \partial_{q_2}) \right) \psi_2^{\text{flat}} \right], \quad (6.31)$$

where the vertex now is

$$F = \epsilon_{ii'}^{s_1}(\mathbf{k}_1) \epsilon_{jj'}^{s_2}(\mathbf{k}_2) t_{ijl} t_{i'j'l'} \left[\sum_{s=\pm} \epsilon_{ll'}^s(\mathbf{p}) \epsilon_{kk'}^s(-\mathbf{p}) \right] \epsilon_{mm'}^{s_3}(\mathbf{k}_3) \epsilon_{nn'}^{s_4}(\mathbf{k}_4) \tilde{t}_{kmn} \tilde{t}_{k'm'n'}, \quad (6.32)$$

with

$$t_{ijl} = \delta_{lj} k_2^i + \delta_{il} p^j + \delta_{ij} k_1^l, \quad \tilde{t}_{ijl} = \delta_{lj} k_3^i + \delta_{il} k_4^j + \delta_{ij} p^l. \quad (6.33)$$

If desired, the sum over polarization tensors can again be re-written as in (6.26). Notice that (6.31) is *not* the only contributions to the graviton quartic wavefunction coefficient and in fact it is not even gauge invariant per se. In the gauge we are working with, namely that of [31], the missing terms are quartic contact contributions resulting from $R^{(3)}$, the square of the extrinsic curvature and the integrating out of the lapse and the shift at second order. We leave a full computation of the missing terms for future work. The application of equation 6.9 and subsequent expansion in terms of differential operators acting on seed functions can be carried out for arbitrary trees.

7 Conclusions and outlook

In this work, we have provided a differential representation of tree-level wavefunction coefficients for massless scalars and gravitons in de Sitter. Our representation is valid for general boost breaking interactions satisfying the bound in (2.1). In Section 6 we have shown how to generalise this representation to cover also gravitational interactions in GR with minimal coupling, which violate (2.1). The differential representation involves purely algebraic operations and so side-steps the need to calculate the nested time integrals that arise in the usual bulk representation based on Feynman-Witten rules. We have provided a series of concrete examples to show how the differential representation is computationally less laborious than the time-integral representation, especially for diagrams with two or more internal propagators. Also, the final result in terms of differential operators takes a relative compact form. On the one hand, this form can already be used for algebraic manipulations. On the other hand, it can be expanded into a fully explicit rational function in a fraction of a second using computer software such as Mathematica. Finally, the differential representation has the property to completely eliminate time from the calculation, which might make it more attune to a potential holographic description of perturbative QFT in de Sitter.

This research can be extended as follows:

- It would be interesting to understand how bulk locality constrains the form of the differential operator that acts on the flat spacetime seed ψ^{flat} to give the dS wavefunction. This might have some relation to the recently discussed manifestly local test [18].
- One should be able to build a minor modification of our construction that computes the wavefunction for boost-breaking interactions of a conformally coupled scalar. Related to this, it would be nice to understand the connection of our procedure to the formalism of the cosmological polytopes of [3, 5, 11].

Acknowledgements

We would like to thank Harry Goodhew, Nima Arkani-Hamed, Sebastian Mizera, and Guilherme Pimentel for useful discussions and S. Jazayeri, M.H.G. Lee, S. Melville and J. Supel for comments on the draft. E.P. has been supported in part by the research program VIDI with Project No. 680-47-535, which is (partly) financed by the Netherlands Organisation for Scientific Research (NWO). This work has been partially supported by STFC consolidated grant ST/T000694/1.

A Derivation of Propagator Relations

Here we derive the propagator relations upon which our analysis rests. Consider the massless propagator in de Sitter and flat space respectively,

$$G(\eta, \eta', k) = \frac{i}{2k^3} [\phi_k^*(\eta)\phi_k(\eta')\theta(\eta - \eta') + \phi_k(\eta)\phi_k^*(\eta')\theta(\eta' - \eta) - \phi_k(\eta)\phi_k(\eta')] , \quad (\text{A.1})$$

$$G_{\text{flat}}(\eta, \eta', k) = \frac{i}{2k} [e^{-ik(\eta-\eta')}\theta(\eta - \eta') + e^{-ik(\eta'-\eta)}\theta(\eta' - \eta) - e^{ik(\eta+\eta')}] , \quad (\text{A.2})$$

where the de Sitter propagator is composed of the massless mode functions

$$\phi_k(\eta) = (1 - ik)e^{ik\eta} . \quad (\text{A.3})$$

Now consider the two time-derivative propagator $G_{\phi'\phi'} = \partial_\eta \partial_{\eta'} G$ integrated against some function $F(\eta, \eta')$

$$\int_{-\infty}^0 d\eta d\eta' F(\eta, \eta') \partial_\eta \partial_{\eta'} G(\eta, \eta', k) . \quad (\text{A.4})$$

When the time derivatives hit both mode functions one gets $k^2 \eta \eta' G_{\text{flat}}(\eta, \eta', k)$. Now we turn to the terms hitting the θ -functions. First we consider terms where a single θ -function is hit. This contributes

$$\frac{2i\delta(\eta - \eta')}{2k} [\phi_k^*(\eta)\partial_{\eta'}\phi_k(\eta') - \phi_k(\eta)\partial_{\eta'}\phi_k^*(\eta')] = -2\eta\eta'\delta(\eta - \eta') . \quad (\text{A.5})$$

Finally, we consider when both θ -functions are hit with the derivative, which gives

$$\int d\eta d\eta' F(\eta, \eta') \frac{i}{2k^3} [\phi_k(\eta)\phi_k^*(\eta')\partial_\eta\delta(\eta' - \eta) - \phi_k^*(\eta)\phi_k(\eta')\partial_\eta\delta(\eta' - \eta)] . \quad (\text{A.6})$$

We now integrate by parts in η . The non-vanishing contribution comes from the derivative hitting the mode functions. This gives us

$$\int d\eta d\eta' F(\eta, \eta') \frac{i}{2k^3} [\phi_k(\eta')\partial_\eta\phi_k^*(\eta) - \phi_k^*(\eta')\partial_\eta\phi_k(\eta)] \delta(\eta - \eta') = \int d\eta d\eta' F(\eta, \eta') [\eta\eta'\delta(\eta - \eta')] . \quad (\text{A.7})$$

Summing the contributions we recover (2.10),

$$\partial_\eta \partial_{\eta'} G(\eta, \eta', k) = \eta\eta' [k^2 G_{\text{flat}}(\eta, \eta', k) - \delta(\eta - \eta')] . \quad (\text{A.8})$$

Now we consider generating the $\phi\phi$ and mixed $\phi'\phi$ de Sitter propagators from the flat space propagator. First note that the mixed propagator $G_{\phi'\phi}$ is

$$\partial_\eta G(\eta, \eta') = \frac{i}{2k} [\eta(1 - ik\eta')e^{-ik(\eta-\eta')}\theta(\eta - \eta') + \eta(1 + ik\eta')e^{-ik(\eta'-\eta)}\theta(\eta' - \eta) - \eta(1 - ik\eta')e^{ik(\eta+\eta')}] . \quad (\text{A.9})$$

Notice that the single-derivative hitting the θ -function vanishes on the support of the δ -function it generates. Given the mode function relation

$$(1 - \eta\partial_\eta)e^{ik\eta} = (1 - ik\eta)e^{ik\eta} , \quad (\text{A.10})$$

we have

$$G_{\phi'\phi} = \partial_\eta G(\eta, \eta', k) = (1 - \eta' \partial_{\eta'}) G_{\text{flat}}(\eta, \eta', k), \quad (\text{A.11})$$

$$G(\eta, \eta') = \frac{1}{k^2} [(1 - \eta \partial_\eta)(1 - \eta' \partial_{\eta'}) G_{\text{flat}}(\eta, \eta', k) + \eta \eta' \delta(\eta - \eta')] , \quad (\text{A.12})$$

where the δ -function in the above expression for G comes from analogous integration by parts manipulations on the term with two derivatives.

References

- [1] A. Adams, N. Arkani-Hamed, S. Dubovsky, A. Nicolis and R. Rattazzi, *Causality, analyticity and an IR obstruction to UV completion*, *JHEP* **10** (2006) 014 [[hep-th/0602178](#)].
- [2] M.F. Paulos, J. Penedones, J. Toledo, B.C. van Rees and P. Vieira, *The S-matrix bootstrap. Part I: QFT in AdS*, *JHEP* **11** (2017) 133 [[1607.06109](#)].
- [3] N. Arkani-Hamed, P. Benincasa and A. Postnikov, *Cosmological Polytopes and the Wavefunction of the Universe*, [1709.02813](#).
- [4] G. Goon, K. Hinterbichler, A. Joyce and M. Trodden, *Shapes of gravity: Tensor non-Gaussianity and massive spin-2 fields*, *JHEP* **10** (2019) 182 [[1812.07571](#)].
- [5] N. Arkani-Hamed and P. Benincasa, *On the Emergence of Lorentz Invariance and Unitarity from the Scattering Facet of Cosmological Polytopes*, [1811.01125](#).
- [6] P. Benincasa, *From the flat-space S-matrix to the Wavefunction of the Universe*, [1811.02515](#).
- [7] N. Arkani-Hamed, D. Baumann, H. Lee and G.L. Pimentel, *The Cosmological Bootstrap: Inflationary Correlators from Symmetries and Singularities*, *JHEP* **04** (2020) 105 [[1811.00024](#)].
- [8] D. Baumann, C. Duaso Pueyo, A. Joyce, H. Lee and G.L. Pimentel, *The Cosmological Bootstrap: Weight-Shifting Operators and Scalar Seeds*, [1910.14051](#).
- [9] C. Sleight, *A Mellin Space Approach to Cosmological Correlators*, *JHEP* **01** (2020) 090 [[1906.12302](#)].
- [10] C. Sleight and M. Taronna, *Bootstrapping Inflationary Correlators in Mellin Space*, *JHEP* **02** (2020) 098 [[1907.01143](#)].
- [11] P. Benincasa, *Cosmological Polytopes and the Wavefunction of the Universe for Light States*, [1909.02517](#).
- [12] A. Bzowski, P. McFadden and K. Skenderis, *Conformal n-point functions in momentum space*, *Phys. Rev. Lett.* **124** (2020) 131602 [[1910.10162](#)].

- [13] D. Baumann, C. Duaso Pueyo, A. Joyce, H. Lee and G.L. Pimentel, *The Cosmological Bootstrap: Spinning Correlators from Symmetries and Factorization*, 2005.04234.
- [14] D. Green and E. Pajer, *On the Symmetries of Cosmological Perturbations*, 2004.09587.
- [15] H. Goodhew, S. Jazayeri and E. Pajer, *The Cosmological Optical Theorem*, 2009.02898.
- [16] C. Sleight and M. Taronna, *From AdS to dS Exchanges: Spectral Representation, Mellin Amplitudes and Crossing*, 2007.09993.
- [17] E. Pajer, *Building a Boostless Bootstrap for the Bispectrum*, *JCAP* **01** (2021) 023 [2010.12818].
- [18] S. Jazayeri, E. Pajer and D. Stefanyszyn, *From Locality and Unitarity to Cosmological Correlators*, 2103.08649.
- [19] H. Isono, H.M. Liu and T. Noumi, *Wavefunctions in dS/CFT revisited: principal series and double-trace deformations*, 2011.09479.
- [20] S. Melville and E. Pajer, *Cosmological Cutting Rules*, *JHEP* **05** (2021) 249 [2103.09832].
- [21] H. Goodhew, S. Jazayeri, M.H. Gordon Lee and E. Pajer, *Cutting Cosmological Correlators*, 2104.06587.
- [22] J. Bonifacio, E. Pajer and D.-G. Wang, *From Amplitudes to Contact Cosmological Correlators*, 2106.15468.
- [23] L. Di Pietro, V. Gorbenko and S. Komatsu, *Analyticity and Unitarity for Cosmological Correlators*, 2108.01695.
- [24] C. Sleight and M. Taronna, *From dS to AdS and back*, 2109.02725.
- [25] M. Hogervorst, J.a. Penedones and K.S. Vaziri, *Towards the non-perturbative cosmological bootstrap*, 2107.13871.
- [26] D. Meltzer, *The Inflationary Wavefunction from Analyticity and Factorization*, 2107.10266.
- [27] C. Sleight and M. Taronna, *On the consistency of (partially-)massless matter couplings in de Sitter space*, 2106.00366.
- [28] S. Céspedes, A.-C. Davis and S. Melville, *On the time evolution of cosmological correlators*, 2009.07874.
- [29] H. Gomez, R.L. Jusinkas and A. Lipstein, *Cosmological Scattering Equations*, 2106.11903.
- [30] G. Cabass, E. Pajer, D. Stefanyszyn and J. Supel, *Bootstrapping Large Graviton non-Gaussianities*, 2109.10189.
- [31] J.M. Maldacena, *Non-Gaussian features of primordial fluctuations in single field inflationary models*, *JHEP* **05** (2003) 013 [astro-ph/0210603].

- [32] D. Anninos, T. Anous, D.Z. Freedman and G. Konstantinidis, *Late-time Structure of the Bunch-Davies De Sitter Wavefunction*, *JCAP* **11** (2015) 048 [1406.5490].
- [33] I. Mata, S. Raju and S. Trivedi, *CMB from CFT*, *JHEP* **07** (2013) 015 [1211.5482].
- [34] A. Bzowski, P. McFadden and K. Skenderis, *Implications of conformal invariance in momentum space*, *JHEP* **03** (2014) 111 [1304.7760].
- [35] N. Kundu, A. Shukla and S.P. Trivedi, *Constraints from Conformal Symmetry on the Three Point Scalar Correlator in Inflation*, *JHEP* **04** (2015) 061 [1410.2606].
- [36] N. Kundu, A. Shukla and S.P. Trivedi, *Ward Identities for Scale and Special Conformal Transformations in Inflation*, *JHEP* **01** (2016) 046 [1507.06017].
- [37] D. Baumann, D. Green, H. Lee and R.A. Porto, *Signs of Analyticity in Single-Field Inflation*, *Phys. Rev.* **D93** (2016) 023523 [1502.07304].
- [38] T. Grall and S. Melville, *Inflation in Motion: Unitarity Constraints in Effective Field Theories with Broken Lorentz Symmetry*, 2005.02366.
- [39] E. Pajer, D. Stefanyszyn and J. Supeł, *The Boostless Bootstrap: Amplitudes without Lorentz boosts*, *JHEP* **12** (2020) 198 [2007.00027].
- [40] D. Stefanyszyn and J. Supeł, *The Boostless Bootstrap and BCFW Momentum Shifts*, 2009.14289.
- [41] T. Grall and S. Melville, *Positivity Bounds without Boosts*, 2102.05683.
- [42] S. Melville and J. Noller, *Positivity in the Sky: Constraining dark energy and modified gravity from the UV*, *Phys. Rev. D* **101** (2020) 021502 [1904.05874].
- [43] D. Stefanyszyn and J. Supeł, *The Boostless Bootstrap and BCFW Momentum Shifts*, *JHEP* **03** (2021) 091 [2009.14289].
- [44] M. Celoria, P. Creminelli, G. Tambalo and V. Yingcharoenrat, *Beyond perturbation theory in inflation*, *JCAP* **06** (2021) 051 [2103.09244].
- [45] P. Creminelli, M.A. Luty, A. Nicolis and L. Senatore, *Starting the Universe: Stable Violation of the Null Energy Condition and Non-standard Cosmologies*, *JHEP* **12** (2006) 080 [hep-th/0606090].
- [46] C. Cheung, P. Creminelli, A.L. Fitzpatrick, J. Kaplan and L. Senatore, *The Effective Field Theory of Inflation*, *JHEP* **03** (2008) 014 [0709.0293].
- [47] L. Bordin, P. Creminelli, A. Khmelnitsky and L. Senatore, *Light Particles with Spin in Inflation*, *JCAP* **10** (2018) 013 [1806.10587].
- [48] S. Endlich, A. Nicolis and J. Wang, *Solid Inflation*, *JCAP* **10** (2013) 011 [1210.0569].

- [49] D. Baumann, W.-M. Chen, C. Duaso Pueyo, A. Joyce, H. Lee and G.L. Pimentel, *Linking the Singularities of Cosmological Correlators*, 2106.05294.
- [50] L. Senatore, K.M. Smith and M. Zaldarriaga, *Non-Gaussianities in Single Field Inflation and their Optimal Limits from the WMAP 5-year Data*, *JCAP* **01** (2010) 028 [0905.3746].
- [51] M. Henningson and K. Skenderis, *The Holographic Weyl anomaly*, *JHEP* **07** (1998) 023 [hep-th/9806087].
- [52] D. Seery, M.S. Sloth and F. Vernizzi, *Inflationary trispectrum from graviton exchange*, *JCAP* **03** (2009) 018 [0811.3934].
- [53] A. Ghosh, N. Kundu, S. Raju and S.P. Trivedi, *Conformal Invariance and the Four Point Scalar Correlator in Slow-Roll Inflation*, *JHEP* **07** (2014) 011 [1401.1426].